nature cell biology

# Control of PKA stability and signalling by the RING ligase praja2

Luca Lignitto[1], Annalisa Carlucci[1], Maria Sepe[1], Eduard Stefan[2], Ornella Cuomo[3], Robert Nisticò[4,5], Antonella Scorziello[3], Claudia Savoia[3], Corrado Garbi[1], Lucio Annunziato[3] and Antonio Feliciello[1,6]

**Activation of G-protein-coupled receptors (GPCRs) mobilizes compartmentalized pulses of cyclic AMP. The main cellular effector of cAMP is protein kinase A (PKA), which is assembled as an inactive holoenzyme consisting of two regulatory (R) and two catalytic (PKAc) subunits. cAMP binding to R subunits dissociates the holoenzyme and releases the catalytic moiety, which phosphorylates a wide array of cellular proteins. Reassociation of PKAc and R components terminates the signal. Here we report that the RING ligase praja2 controls the stability of mammalian R subunits. Praja2 forms a stable complex with, and is phosphorylated by, PKA. Rising cAMP levels promote praja2-mediated ubiquitylation and subsequent proteolysis of compartmentalized R subunits, leading to sustained substrate phosphorylation by the activated kinase. Praja2 is required for efficient nuclear cAMP signalling and for PKA-mediated long-term memory. Thus, praja2 regulates the total concentration of R subunits, tuning the strength and duration of PKA signal output in response to cAMP.**

In higher eukaryotes, essential functions such as neurite growth and morphogenesis, synaptic transmission and hormone production and release require tightly regulated responses to PKA stimulation[1]. Mammalian cells express different classes of PKA holoenzymes whose biological activity depends on the structure and biochemical properties of their R subunits. Catalytic subunits show common kinetic features and substrate specificity. The composition and specific biochemical properties of PKA isoenzymes account, in part, for differential cellular responses to discrete extracellular signals that activate adenylate cyclase[2,3]. Space-restricted kinase activation provides an extra layer of complexity in PKA signalling. PKA is targeted at specific intracellular microdomains through interactions with A-kinase anchor proteins (AKAPs). An AKAP forms a local transduction unit, which includes different signalling/metabolic enzymes, receptors, ion channels, adaptor molecules and messenger RNAs. In this context, the spatio-temporal kinase activation provides a control mechanism to direct, integrate and locally attenuate the cAMP cascade[3–22].

The cAMP–PKA pathway plays a crucial role in synaptic plasticity in a wide variety of species. Pharmacological or genetic inhibition of PKA severely affects the induction of hippocampal long-term potentiation (LTP) and inhibits synaptic plasticity and long-lasting memory[23]. In *Aplysia* sensory neurons, the switch from short-term to long-term facilitation is essential for initiating stable long-term memory. Ubiquitin-dependent proteolysis of R subunits sustains nuclear PKAc signalling and promotes transition from short-term to long-term facilitation, thereby contributing to synaptic strengthening[24–27]. In mammals, proteolysis of R subunits has been linked mechanistically to differentiation and coordinated progression through the cell cycle[28]. However, the identity of the E3 ubiquitin ligase controlling PKA stability in eukaryotes is unknown.

Here, we report the identification of the RING ligase praja2 as the mammalian E3 ligase that targets R subunits to the ubiquitin–proteasome pathway. By binding and degrading R subunits, praja2 sustains ligand-induced activation of PKA, thus coordinating cAMP-mediated activation of PKA downstream of adenylate cyclase.

## RESULTS

### Praja2 is an AKAP

To identify previously unknown PKA-interacting proteins, a rat complementary DNA library was screened by the yeast two-hybrid using mouse full-length RIIα as bait. One positive clone (RBP33) of the screen encoded an open reading frame of 178 amino acids corresponding to residues 531–708 of rat praja2 (also named neurodap1; refs 29,30; Fig. 1a). Praja2 belongs to the family of RING proteins that function as E3 ubiquitin ligases that target cellular substrates for proteasomal degradation[29]. First, we demonstrated that

[1]Dipartimento di Biologia e Patologia Cellulare e Molecolare 'L. Califano', Universitá 'Federico II', 80131 Naples, Italy. [2]Institute of Biochemistry and Center for Molecular Biosciences, University of Innsbruck, 6020 Innsbruck, Austria. [3]Divisione di Farmacologia, Dipartimento di Neuroscienze, Università 'Federico II', 80131 Naples, Italy. [4]Dipartimento Farmacobiologico, Università della Calabria, 87036 Rende, Italy. [5]Laboratorio di Neurologia Sperimentale, IRCCS Fondazione Santa Lucia, 00143 Rome, Italy.
[6]Correspondence should be addressed to A.F. (e-mail: feliciel@unina.it)

Received 13 September 2010; accepted 10 January 2011; published online 20 March 2011; DOI: 10.1038/ncb2209

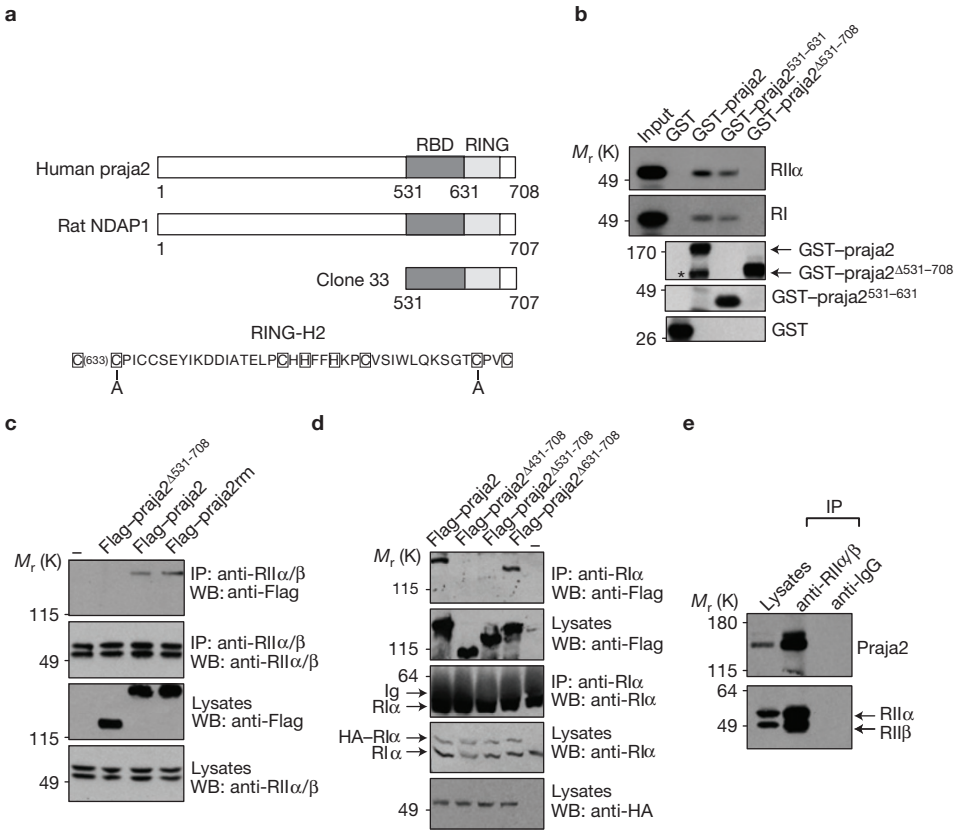


**Figure 1** Praja2 binds to PKA R subunits. (**a**) Schematic representation of human praja2 and its rat homologue neurodap1 (NDAP1, accession no. NP_620251). The cysteine-rich region (RING) and the C-terminal rat clone 33 isolated by the yeast two-hybrid system are shown. RBD, R-binding domain. The sequence of the RING-H2 domain of human praja2 along with the consensus sequence (outlined residues) are shown. Alanine-substituted Cys 634 and Cys 671 are indicated. (**b**) *In vitro* translated, [$^{35}$S]-labelled RIIα and RIα subunits were subjected to pulldown assays with purified GST–praja2, GST–praja2$^{\Delta 531-708}$ and GST–praja2$^{531-631}$ fusions. ∗, proteolytic product. (**c**) Flag–praja2, the RING mutant (C634,671A; praja2rm) or deletion (Δ531–708) mutant were transiently transfected in HEK293 cells. Lysates were immunoprecipitated (IP) with rabbit polyclonal anti-RIIα/β antibody and immunoblotted (WB) with mouse monoclonal anti-Flag and anti-RIIα/β antibodies. (**d**) Flag–praja2 or its deletion mutants (Flag–praja2$^{\Delta 631-708}$, Flag–praja2$^{\Delta 531-708}$ and Flag–praja2$^{\Delta 431-708}$) were expressed, along with HA-tagged RIα, in HEK293 cells. Lysates were subjected to immunoprecipitation with rabbit polyclonal anti-RIα. The precipitates were immunoblotted with the indicated antibodies. (**e**) Lysates (2 mg) from HEK293 cells were subjected to immunoprecipitations using rabbit polyclonal anti-RIIα/β or non-immune IgG. Precipitates were immunoblotted with mouse monoclonal anti-RIIα/β and anti-praja2 antibody. Uncropped images of blots are shown in Supplementary Fig. S8.

praja2 directly interacts with R subunits. Thus, a fusion protein carrying the full-length praja2 appended to the carboxy terminus of glutathione *S*-transferase polypeptide (GST) pulled down *in vitro* translated [$^{35}$S]-labelled R subunits (Fig. 1b). As shown, amino acids 531–631 of praja2 are necessary and sufficient to bind R subunits *in vitro*.

Next, we investigated whether praja2 and R subunits interact in cell extracts. HEK293 cells were transiently transfected with Flag-tagged praja2. As praja2 promotes degradation of R subunits, cells were treated for 15 h with the proteasome inhibitor MG132. Co-immunoprecipitation assays demonstrated that Flag–praja2 and endogenously expressed RIIα/β (Fig. 1c) and RIα (Fig. 1d) subunits form a stable complex. Praja2 ligase activity is not required for RII binding, because a praja2-inactive mutant carrying an alanine substitution of two critical residues within the RING domain (Cys 634 and Cys 671; Flag–praja2rm) binds RII (Fig. 1c). Mapping studies confirmed the role of residues 531–708 of praja2 in mediating the interaction to all R subunits (Fig. 1d). We also detected an endogenous praja2–RII complex (Fig. 1e). PKAc was also present in the praja2 complex, presumably through interaction with the R subunit, because deletion of the R-binding domain of praja2 (residues 531–631) markedly reduced the amount of Flag–praja2 recovered in the PKAc immunoprecipitates (see Supplementary Fig. S1).

Computational sequence analysis predicted the presence of a highly conserved amphipathic α-helix at position 583–600 that may coordinate the binding to R subunits[3–5] (see Supplementary Fig. S2a). As predicted, a synthetic peptide spanning this domain efficiently competed with RIIβ binding to two prototypic PKA-binding proteins, MAP2c (microtubule-associated protein 2c; ref. 31) and AKAP75 (ref. 32; see Supplementary Fig. S2a). A control peptide (carrying proline substitutions) showed no effect. Similarly, disruption of the amphipathic helix of full-length praja2 by proline substitution (A586P, L591P) affected the binding to endogenous RIIα/β subunits (see Supplementary Fig. S2b). The AKAP-binding domain resides at the amino terminus of R subunits (residues 1–30; ref. 3). To test binding of praja2 to the AKAP-binding domain of the R subunit, we carried out GST–praja2 pulldown assays in the presence of a molar excess of a polypeptide containing the R-binding domain of mitochondrial AKAP121 (AKAP121$_{200-450}$). AKAP121$_{200-450}$ competed with praja2 for

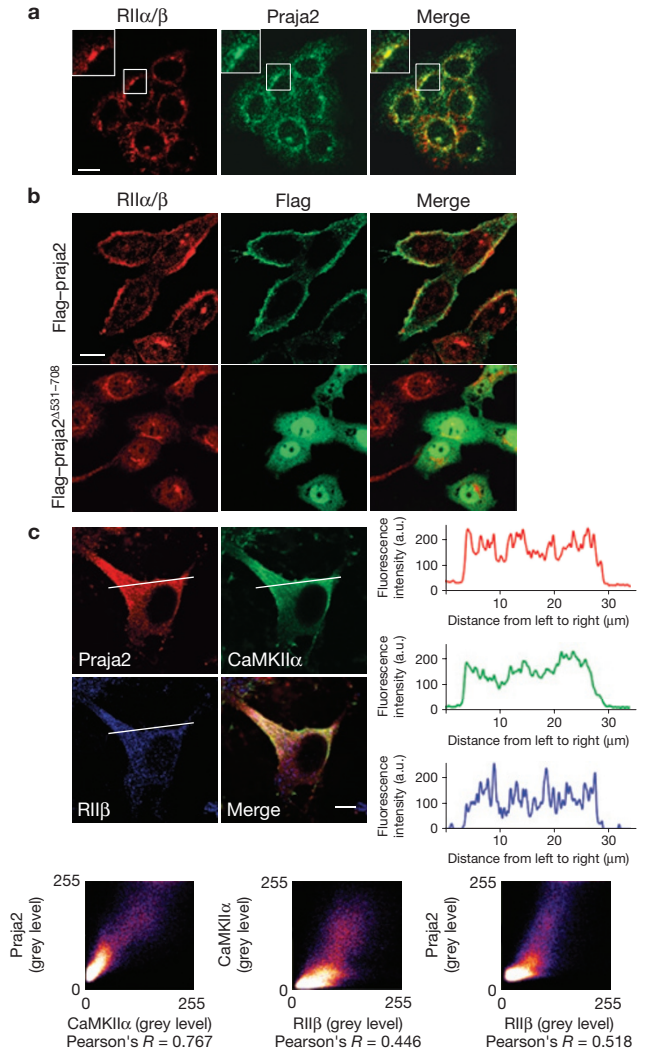


**Figure 2** Praja2 co-localizes with PKA R subunits. (**a**) Human neuroblastoma cells (SHSY) were subjected to double immunostaining with polyclonal anti-praja2 and monoclonal anti-RIIα/β antibodies. Images were collected and analysed by confocal microscopy. The fluorescence signals were quantified by correlation coefficient (Pearson's): $R = 0.51$. Scale bar, 20 μm. Magnification of selected areas is shown (insets). (**b**) SHSY cells were transiently transfected with Flag–praja2 or Flag–praja2$^{\Delta 531-708}$. At 24 h post-transfection, cells were fixed and doubly immunostained with anti-RIIα/β and anti-Flag antibodies. Before collecting, cells were treated with MG132 for 12 h. Images were collected and analysed by confocal microscopy. Flag–praja2/RII, Pearson's coefficient $R = 0.40$; Flag–praja2$^{\Delta 531-708}$/ RII, Pearson's coefficient $R = 0.01$. Scale bar, 20 μm. (**c**) Primary hippocampal neurons were subjected to triple immunofluorescence with rabbit polyclonal anti-praja2, monoclonal mouse anti-CaMKIIα and goat polyclonal anti-RIIβ antibodies. Right panels: profile plots refer to the cross-lines shown in the panels and express the intensity (a.u., arbitrary units) of fluorescence from left to right. Lower panels: Pearson's coefficients between praja2, RIIβ and CaMKIIα. Scale bar, 10 μm.

RII binding (see Supplementary Fig. S2c), indicating that simultaneous RII binding to AKAP121 and praja2 is impossible.

## Praja2 and PKA co-localize in cells and rat brain

*In situ* immunostaining analysis of human neuroblastoma cells demonstrated that endogenous praja2 and RIIα/β subunits partially co-localize inside the cell (Fig. 2a). As praja2 binds R subunits, we formed a hypothesis that overexpression of Flag–praja2 affects intracellular distribution of RIIα/β. To prevent RII degradation by Flag–praja2 overexpression, transfected cells were treated with MG132 before collecting. As suspected, expression of Flag–praja2 redistributed endogenous RIIα/β from the Golgi–centrosome area to the cytoplasm and plasma membrane, and partial co-localization of Flag–praja2 and RIIα/β signals could be detected (Fig. 2b). As a control, we used the praja2 mutant lacking the PKA-binding domain (Flag–praja2$^{\Delta 531-708}$). A similar effect of Flag–praja2 on RIIα/β distribution was also evident in the absence of MG132, although the intensity of RII signal in Flag–praja2-expressing cells was lower when compared with surrounding untransfected cells (see Supplementary Fig. S3a). Green fluorescent protein (GFP)-tagged praja2 also promoted re-localization of RIIα/β subunits from intracellular pools to focal points at the plasma membrane, where the two signals overlapped (Supplementary Fig. S3b, upper panels). No significant changes of RIIα/β localization were evident in cells transfected with GFP (see Supplementary Fig. S3b, lower panels). Expression of Flag–praja2 also redistributed RIα staining (Supplementary Fig. S4). As a control, we used two praja2 mutants lacking the PKA-binding domain (Flag–praja2$^{\Delta 531-708}$ and Flag–praja2$^{\Delta 301-708}$).

We next carried out co-localization studies of endogenous proteins in neurons. Praja2 is widely distributed in neurons of most regions of the mammalian brain and accumulates within cytoplasmic organelles and at postsynaptic densities of axosomatic synapses[30]. Interaction with AKAPs concentrates RIIβ into the soma and dendrites of many types of neuron in the olfactory bulb, basal ganglia, striatum, cerebral cortex and other forebrain regions[8,10,33]. Accordingly, we analysed the distribution patterns of praja2, RIIβ and calmodulin-dependent kinase IIα (CaMKIIα) in different rat brain areas. CaMKIIα is a signalling enzyme abundantly expressed in neurons that selectively defines postsynaptic densities[34]. Praja2 and CaMKIIα have similar expression profiles and intracellular distributions in most of the neurons from different brain regions, including cortex, corpus striatum, hippocampal subregions CA1 and CA3 and dentate gyrus (see Supplementary Fig. S5a). Praja2 is abundantly expressed in pyramidal neurons and in the CA3 region of apical dendrites, whereas RIIβ is present in a few pyramidal neurons and mostly in mossy fibres (see Supplementary Fig. S5b). Moreover, praja2 and RIIβ signals are partly co-distributed in dentate granule cells. Triple immunofluorescence staining demonstrates a partial co-localization of praja2 and RIIβ signals at postsynaptic sites of primary hippocampal neurons (Fig. 2c).

## Praja2 controls the stability of PKA regulatory subunits

We formed a hypothesis that praja2, as an E3 ligase, should destabilize R subunits. To confirm this, HEK293 cells were transiently co-transfected with expression vectors encoding Flag–praja2 (either wild type or RING mutant) and with haemagglutinin (HA)-tagged RIIα (Fig. 3a), Myc–RIIβ (Fig. 3b) or HA–RIα (Fig. 3c). Indeed, wild-type praja2 or a praja2 mutant with alanine-substituted Cys 634 significantly reduced the levels of co-expressed R subunits. In contrast, the concentrations of R subunits in cells expressing Flag–praja2rm were similar to those of control cells. Inhibiting the proteasome with MG132 reversed the praja2-induced degradation

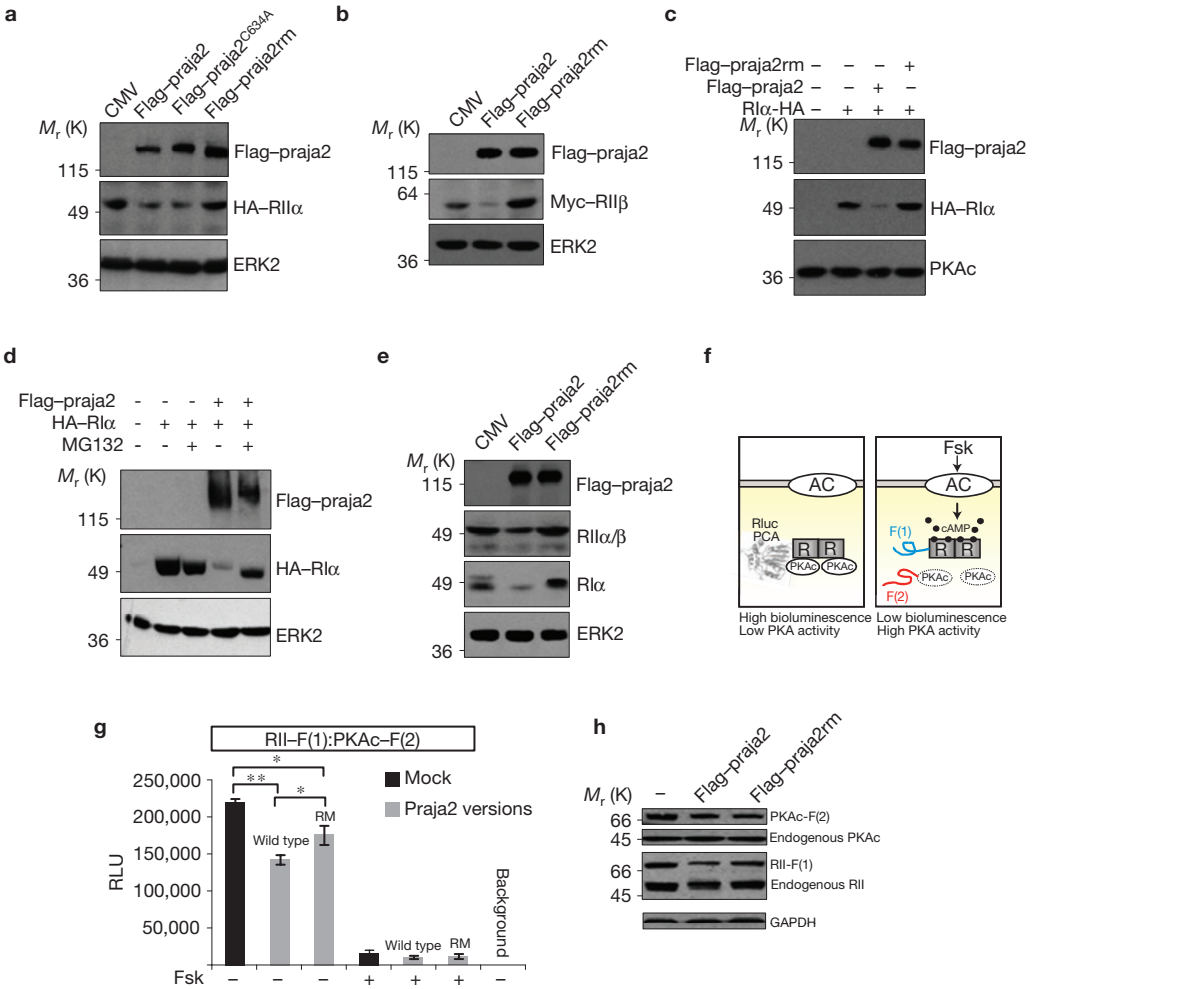


**Figure 3** Praja2 triggers degradation of R subunits. (**a**–**c**) HEK293 cells were transiently co-transfected with HA–RIIα (**a**), Myc–RIIβ (**b**) or HA–RIα (**c**) and Flag–praja2 expression vectors. CMV, cytomegalovirus. In (**a**), two RING mutants were used: praja$^{C634A}$ and Flag–praja2rm. At 24 h post-transfection, cells were collected and lysed. Lysates were immunoblotted with the indicated antibodies. (**d**) The same as in (**c**), except the cells were treated for 8 h with MG132 (20 μM) as indicated before collecting. (**e**) Immunoblot analysis of endogenous R subunits on lysates from cells transiently transfected with Flag–praja2 vectors. Extracellular signal-regulated kinase 2 (ERK2) was used as a loading control. (**f**) Schematic representation of the PCA assay (AC, adenylate cyclase; Fsk, forskolin). (**g**) The effects of praja2 overexpression on PKA heterocomplex formation and dissociation under basal conditions and in response to Fsk (50 μM, 15 min; RLU, relative light units; data are means, ±s.d., $n = 3$). HEK293 cells stably expressing RII–F[1]:PKAc–F[2] (ref. 36) were transiently transfected with Flag–praja2 (Wild type) or Flag–praja2rm (RM). At 24 h post-transfection, the cells were subjected to bioluminescence readout. Statistical significance was assessed using a paired Student *t*-test (∗ $P < 0.05$; ∗∗ $P < 0.01$). (**h**) Comparison of protein expression levels of endogenous and Rluc-PCA-tagged PKA subunits (PKAc, RII) and GAPDH by immunoblotting analysis. Shown is a representative experiment of $n = 3$. Uncropped images of blots are shown in Supplementary Fig. S8.

of RIα subunits (Fig. 3d). Similarly, endogenous RIIα/β and RI subunits were degraded by overexpressed Flag–praja2, but not by Flag–praja2rm (Fig. 3e).

A protein-fragment complementation assay (PCA) based on *Renilla* luciferase (Rluc) was used to assess the impact of praja2 overexpression on formation of the RIIβ:PKAc complex[35,36] (Fig. 3f). This assay can detect dissociation and re-association of the heterodimeric RIIβ and PKAc complex *in vivo*. Under basal conditions, we observed a reduction of PKA complex formation in the presence of functionally active wild-type Flag–praja2, compared with praja2rm (Fig. 3g), further supporting the notion that praja2 promotes the degradation of R subunits. Although equal amounts of expression vectors for PKAc–F[2] and RIIβ–F[1] had been transfected, wild-type praja2 reduced the abundance of RIIβ–F[1] and RIIβ, compared with praja2rm (Fig. 3h).

## Praja2 ubiquitylates PKA regulatory subunits

We next investigated whether praja2 ubiquitylates R subunits. Expression of Flag–praja2, but not of praja2rm, induced accumulation of polyubiquitylated RIIβ (Fig. 4a). As degradation of RIIα/β by praja2 is enhanced by cAMP (see below), we determined whether praja2 was required for RIIα/β ubiquitylation in forskolin (Fsk)-stimulated cells. In control cells, RIIα/β ubiquitylation was potentiated by Fsk and 3-isobutyl-1-methylxanthine (IBMX, phosphodiesterase inhibitor) treatment (Fig. 4b). Depletion of endogenous praja2 markedly reduced RIIα/β ubiquitylation, in both untreated and Fsk-stimulated cells. An *in vitro* ubiquitylation assay confirmed that RIIα is, indeed, a direct substrate of Flag–praja2 (Fig. 4c). In contrast, Flag–praja2rm and a praja2 mutant lacking the PKA phosphorylation sites (Flag–praja2$^{S342A,T389A}$, see below) failed to ubiquitylate RIIα *in vitro*.

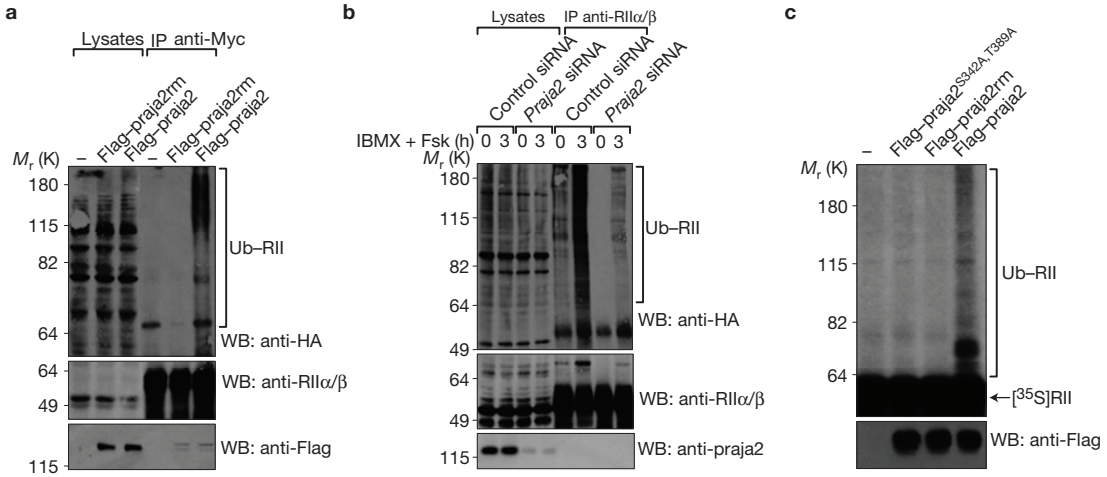


**Figure 4** Praja2 ubiquitylates RIIα/β subunits. (**a**) HEK293 cells were transfected with HA–ubiquitin, RIIβ–Myc and Flag–praja2 or Flag–praja2rm. At 24 h post-transfection, cells were treated with MG132 (20 μM) for 8 h. Lysates were subjected to immunoprecipitations with anti-Myc and immunoblotted with anti-HA, anti-RIIα/β and anti-Flag antibodies. (**b**) HEK293 cells were transfected with HA-tagged ubiquitin. Where indicated, control (control siRNA) or SMARTpool *praja2* siRNA was included in the transfection mix. At 24 h post-transfection, cells were either left untreated or stimulated with Fsk (40 μM) and IBMX (0.5 mM) for 3 h, in the presence of MG132. Lysates were subjected to immunoprecipitations with anti-RIIα/β and immunoblotted with anti-HA, anti-RIIα/β and anti-praja2 antibodies. (**c**) *In vitro* translated, [$^{35}$S]-labelled RIIα was incubated with anti-Flag precipitates (Flag–praja2, Flag–praja2rm or Flag–praja2$^{S342A,T389A}$) isolated from growing cells and 6×His-tagged ubiquitin, in the presence of E1 and UbcH5c (E2). The reaction mix was denatured, size-fractionated by 7% SDS–polyacrylamide gel electrophoresis, and analysed by autoradiography. A fraction of the reaction mixture was immunoblotted with anti-Flag antibody (lower panel). Uncropped images of blots are shown in Supplementary Fig. S8.

## PKA regulates praja2 activity

Ubiquitylation and consequent proteolysis of R subunits by praja2 are stimulated by cAMP, indicating that dissociation of PKA holoenzyme is a prerequisite for R degradation. Regulation of praja2 activity by PKAc might also contribute to the proteolytic turnover of R subunits. To address this issue, we carried out immunostaining analysis of PKAc in cells overexpressing Flag–praja2. Flag–praja2 redistributed PKAc from the Golgi–centrosome area to the cytoplasm and plasma membrane (Fig. 5a). We also carried out co-immunoprecipitation assays to confirm that PKAc interacts with praja2. A Flag–praja2–PKAc complex could be isolated from serum-deprived cells (Fig. 5b). Forskolin treatment increased the amount of PKAc recovered in the anti-Flag precipitates. This effect was reversed by pretreating the cells with H89, a potent PKA inhibitor. In addition, Fsk-triggered complex formation of praja2–PKAc resulted in phosphorylation of praja2 by the associated kinase (Fig. 5b).

Pulldown experiments confirmed that praja2 interacts with PKAc in a cAMP-dependent manner (see Supplementary Fig. S6a). We then carried out an independent test to verify the cAMP-dependent interaction of PKA with praja2 using cAMP-coupled agarose beads that efficiently co-precipitated endogenous PKA holoenzymes from HEK293 cells stably expressing the β2 adrenergic receptor[37] (see Supplementary Fig. S6b and Fig. 5c). The resin-coupled cAMP analogue competes with endogenous cAMP in binding to R subunits, preventing dissociation of PKA holoenzyme by Fsk or isoproterenol treatment. As a negative control, we added excess cAMP (5 mM) to mask the cAMP-binding sites in the R subunits for precipitation (Fig. 5d). Under basal conditions, overexpressed Flag–praja2 (Fig. 5d,e) and praja2rm (Fig. 5f) were co-precipitated with endogenous R–PKAc complexes, consistent with the GST-pulldown experiments (see Supplementary Fig. S6a). However, pretreating the cells with Fsk or isoproterenol for 15 min increased the amount of recovered praja2–PKA complexes (Fig. 5d,e). These results confirm the idea that praja2 forms stable complexes with the PKA holoenzyme and that cAMP elevation further enhances the formation of the PKA–praja2 complex. Ligase activity was dispensable for binding to the R subunit, as a complex containing Flag–praja2rm–PKA subunits (RII and C) could be isolated from cell lysates (Fig. 5f).

We assessed whether praja2 is a substrate of PKAc. Primary sequence analysis predicts the presence of two PKA phosphorylation sites within the core region of praja2 (Ser 342 and Thr 389; Fig. 5g, upper panel). Substitution of both residues with alanine (Flag–praja2$^{S342A,T389A}$) inhibited Fsk-induced praja2 phosphorylation (Fig. 5g, lower panels). *In vitro* kinase assays demonstrated that purified PKAc directly phosphorylates wild-type Flag–praja2, but not the Flag–praja2$^{S342A,T389A}$ mutant, confirming these residues as the main PKA phosphorylation sites (Fig. 5h).

Next, we investigated how praja2 phosphorylation affects PKA binding. Endogenous R–PKAc complexes were precipitated from cell lysates with agarose-coupled 8-(6-aminohexylamino)adenosine-3′,5′-cyclic monophosphorothioate (Rp-8-AHA-cAMP) beads. Under basal conditions, the overexpressed Flag–praja2$^{S342A,T389A}$ mutant co-precipitated with PKA complexes. However, pretreatment of cells with isoproterenol for 15 min decreased complex formation between PKA and the Flag–praja2$^{S342A,T389A}$ mutant (Fig. 5i,j). Co-immunoprecipitation assays confirmed that praja2 phosphorylation is required for its cAMP-mediated interaction with R subunits (Fig. 5k). Moreover, expression of the Flag–praja2$^{S342A,T389A}$ mutant stabilizes RII subunits, even in cells stimulated with Fsk and IBMX (Fig. 5l). We also analysed whether praja2 affects PKA activity by monitoring dissociation and re-association of RII–F[1] and PKAc–F[2] complexes in living cells following Fsk stimulation. Expression of Flag–praja2, Flag–praja2rm or the Flag–praja2$^{S342A,T389A}$ mutant did not affect Fsk-

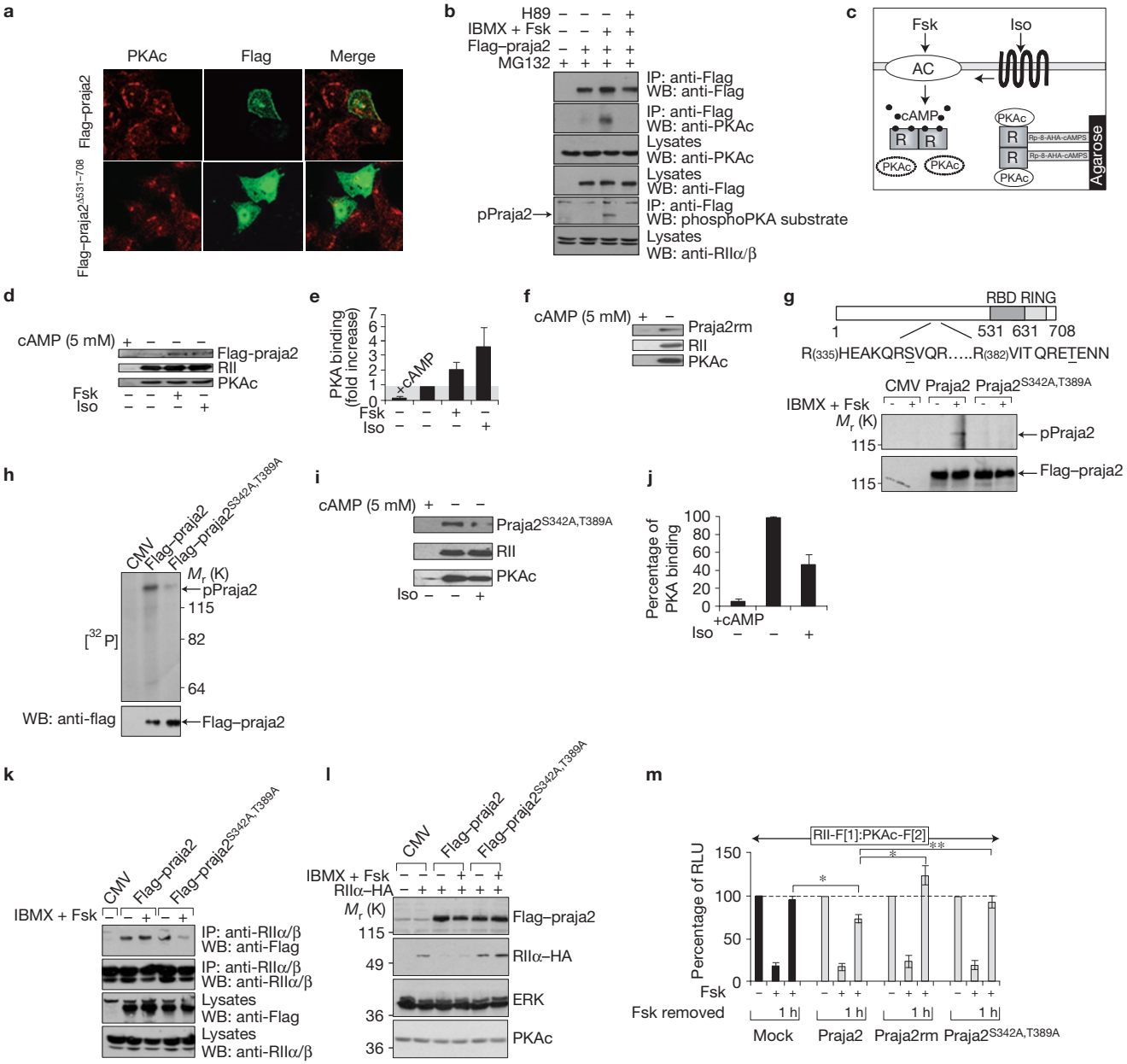


**Figure 5** PKAc binds to and phosphorylates praja2. (**a**) HEK293 cells transiently transfected with Flag–praja2 or Flag–praja2$^{\Delta 531-708}$ vector were immunostained with anti-Flag and anti-PKAc antibodies. Pearson's coefficient: Flag–praja2/PKAc $R = 0.46$ and Flag–praja2$^{\Delta 531-708/}$ PKAc $R = 0.12$. Scale bar, 20 μm. (**b**) Lysates from cells expressing Flag–praja2 and treated with MG132 were immunoprecipitated with anti-Flag antibody. The precipitates were immunoblotted with the indicated antibodies. Where indicated, cells were treated with Fsk (40 μM) and IBMX (0.5 mM) for 30 min ± H89 (10 μM). (**c**) Schematic illustration of the cAMP-precipitation strategy using 8-(6-Aminohexylamino)adenosine-3′,5′-cyclic monophosphorothioate immobilized on agarose (Rp-8-AHA-cAMPS). (**d**) cAMP precipitation of endogenous PKA subunits and Flag–praja2 in response to 15-min treatment with either Fsk (100 μM) or isoproterenol (Iso, 10 μM). In the control, a molar excess of cAMP (5 mM) was added to the lysate. (**e**) Quantitative analysis of the experiments shown in **d** (mean values ± s.e.m. of three independent experiments). (**f**) cAMP precipitation of endogenous PKA subunits and Flag–praja2rm. (**g**) Schematic representation of praja2, including putative PKA consensus sites (Ser 342 and Thr 389, underlined). Lower panels, cells transfected with vectors for Flag–praja2 or Flag–praja2$^{S342A,T389A}$ mutant were serum-deprived overnight and treated with Fsk and IBMX. Flag precipitates were immunoblotted with anti-phosphoSer/Thr PKA substrate antibody. CMV, cytomegalovirus. (**h**) Flag–praja2 and Flag–praja2$^{S342A,T389A}$ mutant were immunoprecipitated from lysates and subjected to an *in vitro* kinase assay. [$^{32}$P]-labelled praja2 was visualized by autoradiography. An aliquot of the samples was immunoblotted with anti-Flag antibody. (**i**) cAMP precipitation of endogenous PKA subunits and Flag–praja2$^{S342A,T389A}$ mutant in response to isoproterenol treatment. (**j**) Complex formation between RII subunits and Flag–praja2$^{S342A,T389A}$ mutant (mean values ± s.e.m. from three independent experiments). (**k**) Co-immunoprecipitation of RIIα/β and Flag–praja2 or Flag–praja2$^{S342A,T389A}$ mutant from cell lysates. (**l**) Immunoblot analysis of cell lysates expressing HA–RIIα and Flag–praja2 or Flag–praja2$^{S342A,T389A}$. (**m**) U2OS cells transfected with vectors for RII–F[1], PKAc–F[2] and Flag–praja2 versions were treated with ±50 μM Fsk for 30 min.The forskolin was washed out and cells were harvested 1 h later. Shown are the effects of praja2 on PKA holoenzyme dissociation and re-association. The untreated sample was set as 100% (RLU, relative light units; $n = 3$ independent experiments; ± s.e.m.). Statistical significance was assessed using a paired Student *t*-test (∗ $P < 0.05$; ∗∗ $P < 0.01$). Uncropped images of blots are shown in Supplementary Fig. S8.

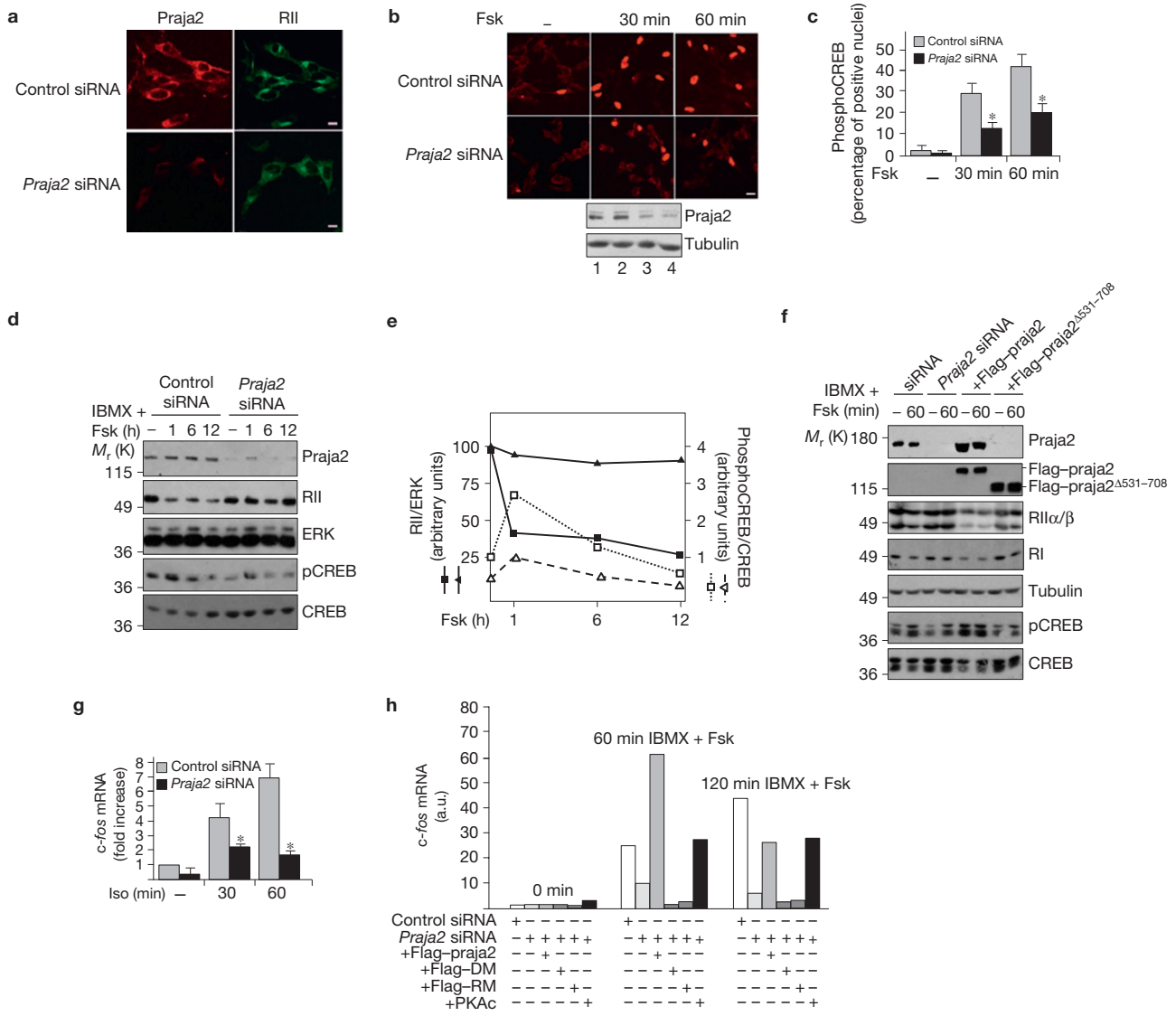


**Figure 6** Praja2 controls PKA signalling in cells. (**a**) Double immunofluorescence for praja2 and RIIβ in human neuroblastoma cells (SHSY) transiently transfected with control siRNA or *praja2* siRNA. Scale bar, 20 μm. (**b**) At 24 h post-transfection, cells were serum deprived overnight and stimulated with Fsk (40 μM) and IBMX (0.5 mM) for 30 and 60 min. Formalin-fixed cells were immunostained with anti-phosphoSer-133 antibody. Immunoblots (lower panels) show the expression of praja2 in control siRNA (lanes 1, 2) and *praja2*-siRNA-transfected (lanes 3, 4) cells, left untreated (lanes 1, 3) or stimulated with Fsk for 60 min (lanes 2, 4). Scale bar, 30 μm. (**c**) Quantitative analysis of the experiments shown in **b**. The data are expressed as the mean ± s.e.m. of three independent experiments carried out in triplicate. A total of 200–250 cells were scored in each set of experiments. $*P < 0.01$ versus control (siRNAc). (**d**) Lysates from control siRNA- or *praja2*-siRNA-transfected cells were serum deprived overnight. Before collecting, cells were left untreated or stimulated with Fsk and IBMX for the indicated times. Lysates were immunoblotted with the indicated antibodies. (**e**) Quantitative analysis of the experiment shown in **d**. A mean of two independent experiments that gave similar results is shown. Squares, control siRNA; triangles, *praja2* siRNA. (**f**) Immunoblot analysis of lysates from control (siRNAc) or *praja2*-siRNA (3′UTR)-transfected cells. Before collecting, cells were serum deprived overnight and left untreated or stimulated with Fsk and IBMX for 60 min. Where indicated, Flag–praja2 and Flag–praja2$^{\Delta 531-708}$ vectors were included in the transfection mixture. (**g**,**h**) Quantitative PCR with reverse transcription showing c-*fos* accumulation in cells transfected with control siRNA or *praja2* siRNA and stimulated with isoproterenol (1 μM; **g**) or Fsk (40 μM) and IBMX (0.5 mM; **h**) for the indicated times. The data represent a mean value ± s.e.m. from three (**g**) or two (**h**) independent experiments carried out in triplicate. Where indicated, vectors for Flag–praja2, Flag–praja2$^{S342A,T389A}$ mutant (double mutant, DM), Flag–praja2rm (RM) and PKAc were included in the transfection mixture. $*P < 0.01$ versus control (siRNAc). Uncropped images of blots are shown in Supplementary Fig. S8.

induced dissociation of PKA holoenzyme (Fig. 5m). However, during the recovery phase (1 h following Fsk removal), wild-type Flag–praja2, but not praja2rm or the Flag–praja2$^{S342A,T389A}$ mutant, significantly reduced the reconstitution of the PKA holoenzyme. This implies that PKA activity regulates the abundance of compartmentalized pools of R subunits through praja2 phosphorylation and recruitment to R subunits, leading to subsequent R proteolysis.

## Praja2 controls PKA-dependent CREB phosphorylation and c-*fos* transcription

The coupling of adenylate cyclase activation at the cell membrane to mRNA induction involves dissociation of PKA holoenzyme, translocation of PKAc to the nucleus, phosphorylation of the transcription factor CREB (cAMP response element binding protein) at Ser 133 and phosphoCREB/co-activator-dependent activation of

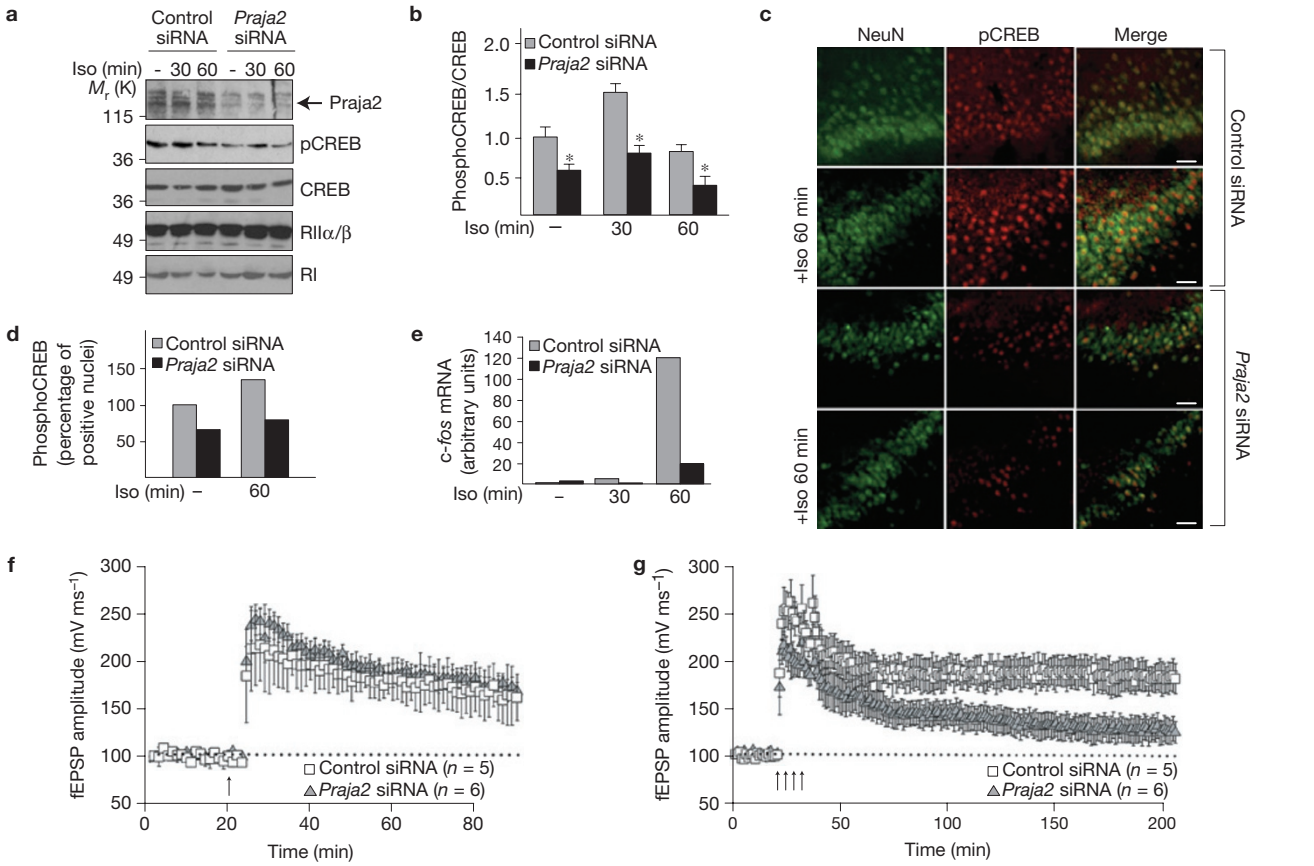


**Figure 7** Praja2 controls PKA signalling and LTP in rat brain. (**a**) Immunoblot analysis of lysates from hippocampal/striatal regions of rat brain intraventricularly perfused with siRNAs and subsequently treated with isoproterenol for the indicated times. (**b**) Quantitative analysis of phosphoCREB from the experiments shown in **a**. The data are expressed as the mean ± s.e.m. of three experiments. $*P < 0.05$ versus control. (**c**) Sections from hippocampal subregion CA1 of rat brain perfused with siRNAs and treated with isoproterenol as in **a** were doubly immunostained with anti-phosphoCREB and anti-NeuN antibodies. The images were collected and analysed by confocal microscopy. Scale bar, 50 μm. (**d**) Quantitative analysis of the experiments shown in **c**. The data are expressed as the means of two independent experiments that gave similar results. A total of 300–350 cells were scored in each set of experiments. (**e**) Quantitative PCR with reverse transcription showing c-*fos* accumulation in the striatum. The data represent a mean value from two independent experiments made in duplicate that gave similar results. (**f**) E-LTP induced by one train of HFS is comparable between control siRNA (white squares, $n = 5$) and *praja2*-siRNA rats (grey triangles, $n = 6$). Field excitatory postsynaptic potential (fEPSP) amplitudes are expressed as percentages of the pretetanus baseline. The data are expressed as the mean ± s.e.m. (**g**) A TBS protocol elicits normal L-LTP in control siRNA rats (white squares, $n = 5$), but deficient L-LTP in *praja2*-siRNA rats (grey triangles, $n = 6$). Uncropped images of blots are shown in Supplementary Fig. S8.

nuclear gene transcription[11,38,39]. The data shown above indicate that praja2 mediates cAMP-dependent degradation of R subunits, prolonging the time of PKAc activation. Thus, we would predict that depletion of praja2 decreases PKAc signalling to nuclear targets (that is, CREB). Endogenous praja2 was depleted by transfecting short interfering RNA against praja2 (*praja2* siRNA), as confirmed by immunofluorescence microscopy (Fig. 6a) and immunoblot analyses (Fig. 6b, lower panels). In control cells, most RII staining was concentrated at the Golgi–centrosome area and the perinuclear region. praja2 downregulation dispersed RIIβ throughout the cytoplasm (Fig. 6a). The physiological significance of praja2 downregulation for nuclear cAMP signalling was evaluated by analysis of CREB phosphorylation at Ser 133 *in situ*. In control cells, Fsk stimulation increased the number of phosphoSer-133-CREB-positive nuclei in a time-dependent manner (Fig. 6b,c). In contrast, a nearly twofold decline in phosphoSer-133-CREB-positive nuclei was seen in cells transfected with *praja2* siRNA at both time points of Fsk stimulation. Downregulation of praja2 by *praja2* siRNA prevented the Fsk-induced decline of RII subunits and inhibited CREB phosphorylation (Fig. 6d,e). Co-expression of Flag–praja2, but not of its deletion mutant (Flag–praja2$^{\Delta 531-708}$), reversed the effects of *praja2* siRNA (Fig. 6f).

Transcription of c-*fos* is mediated by binding of CREB to an upstream cAMP-responsive element (CRE). CREB phosphorylation at Ser 133 drives c-*fos* transcription[39]. We monitored the effects of praja2 downregulation on c-*fos* mRNA synthesis. In control (siRNAc) cells, low levels of c-*fos* mRNA were detected under basal conditions. Activation of adenylate cyclase by isoproterenol induced a robust and persistent increase of c-*fos* mRNA at 30 and 60 min following treatment (Fig. 6g). Induction of c-*fos* mRNA was reduced several-fold in *praja2*-siRNA-transfected cells. Similar effects on c-*fos* transcription by *praja2* siRNA were observed in cells that were stimulated with Fsk (Fig. 6h). Rescue experiments confirmed the role of praja2 phosphorylation and activity in the control of cAMP-induced gene transcription. Thus, co-expression of wild-type Flag–praja2, but not of its mutants (Flag–praja2rm and Flag–praja2$^{S342A,T389A}$), rescued c-*fos* mRNA accumulation in *praja2*-siRNA-transfected cells, at both 60 and 120 min of stimulation with Fsk (Fig. 6h). Moreover, co-expression of PKAc bypassed the block imposed by *praja2* siRNA

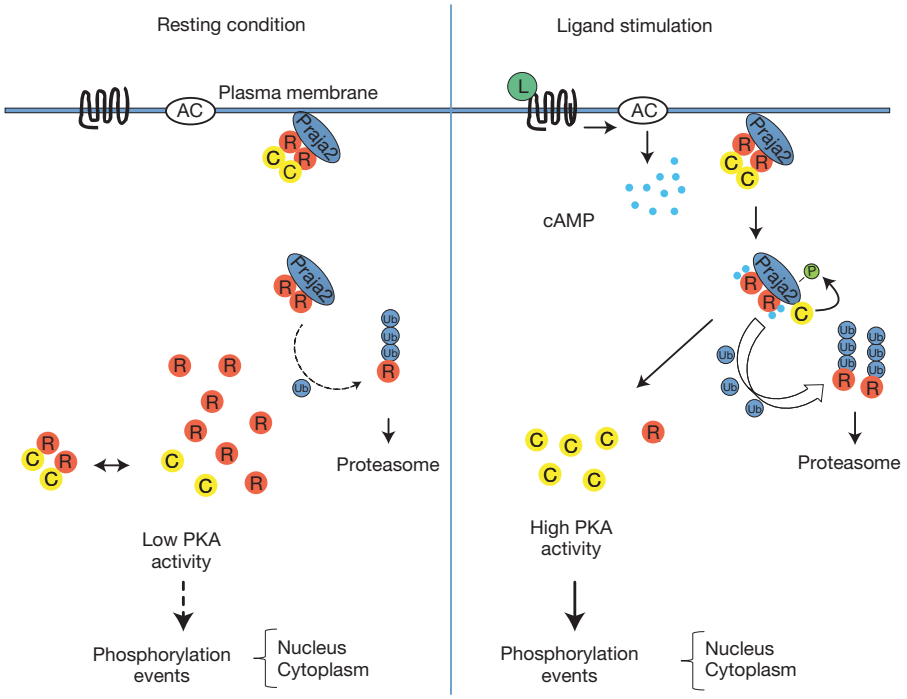


**Figure 8** Schematic representation of the role of praja2 in PKA signalling. Under resting conditions, the inactive PKA holoenzyme accumulates inside the cells as a consequence of the low ubiquitylation rate of R subunits. Elevation of intracellular cAMP levels by ligand (L) stimulation of the adenylate cyclase (AC) efficiently activates PKA, which in turn phosphorylates praja2. Phosphorylated praja2 ubiquitylates and degrades R subunits through the proteasome pathway. Accumulation of free, active PKAc (C) sustains substrate phosphorylation and positively impacts on the amplitude and duration of cAMP signalling.

and partially restored c-*fos* levels (Fig. 6h). These findings indicate that downregulation of R subunits by praja2 prolongs the wave of PKAc activation and positively impacts on downstream signalling. To provide further evidence for this, we monitored c-*fos* mRNA accumulation in cells that were depleted of RIIα/β subunits, a condition that would mimic RII degradation induced by praja2. As predicted, downregulation of RIIα/β subunits significantly increased c-*fos* mRNA levels in Fsk-stimulated cells (see Supplementary Fig. S7a). The effects of RIIα/β subunits on c-*fos* mRNA accumulation were reversed by co-expressing exogenous RIIα/β subunits.

### Praja2 is required for PKA signalling and LTP in rat brain

Praja2 is abundantly expressed in mammalian brain[30]. This prompted us to investigate whether downregulation of praja2 in intact brains affects nuclear PKAc signalling. *Praja2* siRNA or control siRNA were perfused intracerebro-ventricularly in rats (see Supplementary Fig. S7b). Intracerebral infusions of *praja2* siRNA reduced praja2 levels in the areas surrounding the perfused hemispheres (striatum and hippocampus) (Fig. 7a). Functional consequences of praja2 downregulation on PKA signalling were evaluated by CREB phosphorylation and c-*fos* transcription in striato-hippocampal areas. Significant amounts of basal phosphoSer-133-CREB were evident in control rat brain (Fig. 7a,b). CREB phosphorylation modestly increased at 30 min after intracerebro-ventricular infusion of isoproterenol and declined in the next 30 min. *In vivo* silencing of praja2 reduced CREB phosphorylation by about half, both under basal conditions and with isoproterenol treatment. *In situ* immunohistochemistry confirmed the inhibition of CREB phosphorylation in the hippocampal area of *praja2*-siRNA-perfused rat brain, compared with controls (Fig. 7c,d). Inhibition of CREB phosphorylation by *praja2* siRNA provoked a significant downregulation of isoproterenol-induced c-*fos* transcription (Fig. 7e).

Finally, we investigated the electrophysiological consequences of praja2 downregulation by monitoring LTP at perforant pathway–dentate gyrus granule-cell synapses. First, we studied the early, PKA-independent, phase of LTP (E-LTP) induced by one train of high-frequency stimulation (HFS; ref. 40). We found similar E-LTP in both control siRNA- and *praja2*-siRNA-treated rats (50–60 min post-HFS: control siRNA, 155 ± 21%; *praja2*-siRNA, 161 ± 9%, $P > 0.05$; Fig. 7f). Next, we studied the late phase of LTP (L-LTP), which typically requires the activation of cAMP–PKA (ref. 40), by using a theta burst stimulation (TBS) pattern. Interestingly, this protocol reliably induced sustained L-LTP in controls, but not in *praja2*-siRNA-treated rats (150–160 min post-TBS: control siRNA, 177 ± 11%; *praja2*-siRNA, 123 ± 11%, $P < 0.05$; Fig. 7g). These results indicate that praja2 activity is essential for long-term memory processes.

## DISCUSSION

We report the identification of praja2 as the E3 ligase responsible for ubiquitylation and proteolysis of PKA regulatory subunits (RI and RII). Praja2 acts as an AKAP that binds RI/RII subunits and positions the holoenzymes at the cell membrane, perinuclear region and cellular organelles. Mapping analysis revealed the presence of an amphipathic helix located at the C terminus of praja2 that mediates interaction to R subunits. Co-localization of praja2–PKA complexes with PKA substrate/effector molecules ensures efficient integration and

propagation of the locally generated cAMP to distinct target sites. In the course of cAMP stimulation, praja2 optimally transfers ubiquitin molecules to dissociated R subunits. Degradation of ubiquitylated R subunits by the proteasome sustains downstream PKAc signalling and significantly impacts on specialized cell functions.

Activation of PKA is rapidly followed by a refractory period during which ligand-stimulated cells become less responsive to the next cAMP wave. Phosphodiesterases, Ser/Thr phosphatases and transcriptional regulation of components of the cAMP signalling cascade control the establishment and maintenance of the refractory period[41–43]. In this regard, the relative abundance of R and PKAc subunits contributes to the strength and duration of cAMP signalling. For example, increased PKAc activity profoundly alters the sensitivity of cells to ligand stimulation, sustaining downstream cAMP signalling and impacting on different aspects of cellular behaviour[44,45]. Deletion of the PKA RIIβ subunit in mice enhances basal activity of PKAc subunits, leading to an increased metabolic rate in adipose tissue and impairment of neuronal activities[46,47]. In *Aplysia* sensory neurons, ubiquitin-dependent proteolysis of R subunits facilitates downstream PKAc signalling and controls induction and consolidation of long-term memory[26,48]. However, the E3 ubiquitin ligase controlling the stability of R subunits in eukaryotes was unknown.

We have identified praja2 as the E3 ligase that ubiquitylates and targets mammalian R subunits for degradation. praja2–PKA complexes optimally decode signals generated at cell membranes and rapidly propagate the cAMP input to the downstream effector kinase. Overexpression of praja2 induces proteolysis of R subunits, whereas genetic knockdown of the ligase prevents cAMP-induced decline of R subunit levels. Under basal conditions, praja2 controls the bulk levels of compartmentalized PKA holoenzyme. Elevation of cAMP levels increases praja2–PKA complex formation, favouring efficient and synchronized local activation of the kinase. Phosphorylation of praja2 by PKAc enhances proteolysis of R subunits and reduces the stoichiometric ratio of R/PKAc, leading to sustained substrate phosphorylation by the activated kinase (Fig. 8). The molecular events controlled by praja2 ultimately impact on the amplitude and duration of PKA signalling (that is, CREB phosphorylation and nuclear gene transcription) and significantly contribute to synaptic plasticity and long-term memory.

Collectively, our findings indicate that PKA-regulated proteolysis of R subunits by praja2 constitutes an important positive-feedback mechanism that controls the rate and magnitude of cAMP–PKA signalling. Understanding the intricate connection between hormone-generated signals and the ubiquitin–proteasome pathway, and identifying the mechanism(s) underlying cAMP signal generation and attenuation at target sites, provides basic insights into hormone action. □

## METHODS

Methods and any associated references are available in the online version of the paper at http://www.nature.com/naturecellbiology/

*Note: Supplementary Information is available on the Nature Cell Biology website*

### ACKNOWLEDGEMENTS

This work was supported by Grants from Associazione Italiana per la Ricerca sul Cancro (AIRC) and the Italian Ministry of University and Research (MIUR) 2008–2009 (2007KS47FW_002). E.S. was supported from Austrian Science Fund (FWF) Grant P22608 and Junior Researcher Support 2009 (University of Innsbruck). Special thanks to M. Gottesman, E. Avvedimento and K. Bister for discussion and critical reading of the manuscript, D. Viaggiano for help in immunohistochemistry and confocal microscopy analysis, R. D. Donne for help in carrying out experiments and S. McKnight and M. Ginsberg for providing the vectors for epitope-tagged R subunits. This manuscript is dedicated to the memory of M. Graziano.

### AUTHOR CONTRIBUTIONS

L.L., L.A., E.S. and A.F. designed the experiments. L.L. carried out most of the experiments except for the following: Figs 2c, 7c,d and Supplementary Figs S5 and S7b were carried out by A.S., C.S. and O.C. Figs 1d and 5g were carried out by M.S., who also generated praja2-deletion mutants. Figs 3f–h, 5c–f, i, j, m and Supplementary Fig. S6b were carried out by E.S. Figs 2a,b, 5a, 6a and Supplementary Figs S3 and S4 were carried out by C.G. Figs 6g,h, 7e and Supplementary Fig. S7a were carried out by A.C. Fig. 7f,g were carried out by R.N. L.L., E.S., L.A. and A.F. analysed the data. A.F. wrote the manuscript with contributions from L.A. and E.S.

### COMPETING FINANCIAL INTERESTS

The authors declare no competing financial interests.

Published online at http://www.nature.com/naturecellbiology
Reprints and permissions information is available online at http://npg.nature.com/reprintsandpermissions/

1. Taylor, S. S. *et al.* Signaling through cAMP and cAMP-dependent protein kinase: diverse strategies for drug design. *Biochim. Biophys. Acta* **1784,** 16–26 (2008).
2. Amieux, P. S. & McKnight, G. S. The essential role of RI α in the maintenance of regulated PKA activity. *Ann. NY Acad. Sci.* **968,** 75–95 (2002).
3. Feliciello, A., Gottesman, M. E. & Avvedimento, E. V. The biological functions of A-kinase anchor proteins. *J. Mol. Biol.* **308,** 99–114 (2001).
4. Tasken, K. & Aandahl, E. M. Localized effects of cAMP mediated by distinct routes of protein kinase A. *Physiol. Rev.* **84,** 137–167 (2004).
5. Beene, D. L. & Scott, J. D. A-kinase anchoring proteins take shape. *Curr. Opin. Cell Biol.* **19,** 192–198 (2007).
6. Dell'Acqua, M. L. *et al.* Regulation of neuronal PKA signaling through AKAP targeting dynamics. *Eur. J. Cell Biol.* **85,** 627–633 (2006).
7. Dessauer, C. W. Adenylyl cyclase–A-kinase anchoring protein complexes: the next dimension in cAMP signaling. *Mol. Pharmacol.* **76,** 935–941 (2009).
8. Zhong, H. *et al.* Subcellular dynamics of type II PKA in neurons. *Neuron* **62,** 363–374 (2009).
9. Carlucci, A., Lignitto, L. & Feliciello, A. Control of mitochondria dynamics and oxidative metabolism by cAMP, AKAPs and the proteasome. *Trends Cell Biol.* **18,** 604–613 (2008).
10. Tunquist, B. J. *et al.* Loss of AKAP150 perturbs distinct neuronal processes in mice. *Proc. Natl Acad. Sci. USA* **105,** 12557–12562 (2008).
11. Feliciello, A., Li, Y., Avvedimento, E. V., Gottesman, M. E. & Rubin, C. S. A-kinase anchor protein 75 increases the rate and magnitude of cAMP signaling to the nucleus. *Curr. Biol.* **7,** 1011–1014 (1997).
12. Harada, H. *et al.* Phosphorylation and inactivation of BAD by mitochondria-anchored protein kinase A. *Mol. Cell* **3,** 413–422 (1999).
13. Feliciello, A., Gottesman, M. E. & Avvedimento, E. V. cAMP-PKA signaling to the mitochondria: protein scaffolds, mRNA and phosphatases. *Cell Signal.* **17,** 279–287 (2005).
14. Gomez, L. L., Alam, S., Smith, K. E., Horne, E. & Dell'Acqua, M. L. Regulation of A-kinase anchoring protein 79/150-cAMP-dependent protein kinase postsynaptic targeting by NMDA receptor activation of calcineurin and remodeling of dendritic actin. *J. Neurosci.* **22,** 7027–7044 (2002).
15. Houslay, M. D. Underpinning compartmentalised cAMP signalling through targeted cAMP breakdown. *Trends Biochem. Sci.* **35,** 91–100 (2010).
16. Willoughby, D., Wong, W., Schaack, J., Scott, J. D. & Cooper, D. M. An anchored PKA and PDE4 complex regulates subplasmalemmal cAMP dynamics. *EMBO J.* **25,** 2051–2061 (2006).
17. Smith, F. D. *et al.* AKAP-Lbc enhances cyclic AMP control of the ERK1/2 cascade. *Nat. Cell Biol.* **12,** 1242–1249 (2010).
18. Jurado, S., Biou, V. & Malenka, R. C. A calcineurin/AKAP complex is required for NMDA receptor-dependent long-term depression. *Nat. Neurosci.* **13,** 1053–1055 (2010).
19. Mauban, J. R., O'Donnell, M., Warrier, S., Manni, S. & Bond, M. AKAP-scaffolding proteins and regulation of cardiac physiology. *Physiology (Bethesda)* **24,** 78–87 (2009).
20. Bhattacharyya, S., Biou, V., Xu, W., Schluter, O. & Malenka, R. C. A critical role for PSD-95/AKAP interactions in endocytosis of synaptic AMPA receptors. *Nat. Neurosci.* **12,** 172–181 (2009).
21. Lim, C. J. *et al.* α4 integrins are type I cAMP-dependent protein kinase-anchoring proteins. *Nat. Cell Biol.* **9,** 415–421 (2007).
22. Carlucci, A. *et al.* Proteolysis of AKAP121 regulates mitochondrial activity during cellular hypoxia and brain ischaemia. *EMBO J.* **27,** 1073–1084 (2008).

23. Huang, Y. Y. & Kandel, E. R. Recruitment of long-lasting and protein kinase A-dependent long-term potentiation in the CA1 region of hippocampus requires repeated tetanization. *Learn. Mem.* **1,** 74–82 (1994).
24. Chain, D. G. *et al.* Mechanisms for generating the autonomous cAMP-dependent protein kinase required for long-term facilitation in Aplysia. *Neuron* **22,** 147–156 (1999).
25. Chain, D. G., Hegde, A. N., Yamamoto, N., Liu-Marsh, B. & Schwartz, J. H. Persistent activation of cAMP-dependent protein kinase by regulated proteolysis suggests a neuron-specific function of the ubiquitin system in Aplysia. *J. Neurosci.* **15,** 7592–7603 (1995).
26. Chain, D. G., Schwartz, J. H. & Hegde, A. N. Ubiquitin-mediated proteolysis in learning and memory. *Mol. Neurobiol.* **20,** 125–142 (1999).
27. Hegde, A. N. *et al.* Ubiquitin C-terminal hydrolase is an immediate-early gene essential for long-term facilitation in Aplysia. *Cell* **89,** 115–126 (1997).
28. Feliciello, A. *et al.* The localization and activity of cAMP-dependent protein kinase affect cell cycle progression in thyroid cells. *J. Biol. Chem.* **275,** 303–311 (2000).
29. Yu, P., Chen, Y., Tagle, D. A. & Cai, T. PJA1, encoding a RING-H2 finger ubiquitin ligase, is a novel human X chromosome gene abundantly expressed in brain. *Genomics* **79,** 869–874 (2002).
30. Nakayama, M., Miyake, T., Gahara, Y., Ohara, O. & Kitamura, T. A novel RING-H2 motif protein downregulated by axotomy: its characteristic localization at the postsynaptic density of axosomatic synapse. *J. Neurosci.* **15,** 5238–5248 (1995).
31. Rubino, H. M., Dammerman, M., Shafit-Zagardo, B. & Erlichman, J. Localization and characterization of the binding site for the regulatory subunit of type II cAMP-dependent protein kinase on MAP2. *Neuron* **3,** 631–638 (1989).
32. Bregman, D. B., Hirsch, A. H. & Rubin, C. S. Molecular characterization of bovine brain P75, a high affinity binding protein for the regulatory subunit of cAMP-dependent protein kinase II β. *J. Biol. Chem.* **266,** 7207–7213 (1991).
33. Glantz, S. B., Amat, J. A. & Rubin, C. S. cAMP signaling in neurons: patterns of neuronal expression and intracellular localization for a novel protein, AKAP 150, that anchors the regulatory subunit of cAMP-dependent protein kinase II β. *Mol. Biol. Cell* **3,** 1215–1228 (1992).
34. Zhou, Y. *et al.* Interactions between the NR2B receptor and CaMKII modulate synaptic plasticity and spatial learning. *J. Neurosci.* **27,** 13843–13853 (2007).
35. Michnick, S. W., Ear, P. H., Manderson, E. N., Remy, I. & Stefan, E. Universal strategies in research and drug discovery based on protein-fragment complementation assays. *Nat. Rev. Drug Discov.* **6,** 569–582 (2007).
36. Stefan, E. *et al.* Quantification of dynamic protein complexes using *Renilla* luciferase fragment complementation applied to protein kinase A activities *in vivo*. *Proc. Natl Acad. Sci. USA* **104,** 16916–16921 (2007).
37. Lavoie, C. *et al.* β1/β2-adrenergic receptor heterodimerization regulates β 2-adrenergic receptor internalization and ERK signaling efficacy. *J. Biol. Chem.* **277,** 35402–35410 (2002).
38. Lonze, B. E. & Ginty, D. D. Function and regulation of CREB family transcription factors in the nervous system. *Neuron* **35,** 605–623 (2002).
39. Montminy, M. Transcriptional regulation by cyclic AMP. *Annu. Rev. Biochem.* **66,** 807–822 (1997).
40. Malleret, G. *et al.* Bidirectional regulation of hippocampal long-term synaptic plasticity and its influence on opposing forms of memory. *J. Neurosci.* **30,** 3813–3825 (2010).
41. Armstrong, R., Wen, W., Meinkoth, J., Taylor, S. & Montminy, M. A refractory phase in cyclic AMP-responsive transcription requires down regulation of protein kinase A. *Mol. Cell Biol.* **15,** 1826–1832 (1995).
42. Canettieri, G. *et al.* Attenuation of a phosphorylation-dependent activator by an HDAC–PP1 complex. *Nat. Struct. Biol.* **10,** 175–181 (2003).
43. Houslay, M. D., Baillie, G. S. & Maurice, D. H. cAMP-specific phosphodiesterase-4 enzymes in the cardiovascular system: a molecular toolbox for generating compartmentalized cAMP signaling. *Circ. Res.* **100,** 950–966 (2007).
44. Davis, G. W., DiAntonio, A., Petersen, S. A. & Goodman, C. S. Postsynaptic PKA controls quantal size and reveals a retrograde signal that regulates presynaptic transmitter release in *Drosophila*. *Neuron* **20,** 305–315 (1998).
45. Amieux, P. S. *et al.* Increased basal cAMP-dependent protein kinase activity inhibits the formation of mesoderm-derived structures in the developing mouse embryo. *J. Biol. Chem.* **277,** 27294–27304 (2002).
46. Newhall, K. J., Cummings, D. E., Nolan, M. A. & McKnight, G. S. Deletion of the RIIβ-subunit of protein kinase A decreases body weight and increases energy expenditure in the obese, leptin-deficient ob/ob mouse. *Mol. Endocrinol.* **19,** 982–991 (2005).
47. Cummings, D. E. *et al.* Genetically lean mice result from targeted disruption of the RII β subunit of protein kinase A. *Nature* **382,** 622–626 (1996).
48. Hegde, A. N., Goldberg, A. L. & Schwartz, J. H. Regulatory subunits of cAMP-dependent protein kinases are degraded after conjugation to ubiquitin: a molecular mechanism underlying long-term synaptic plasticity. *Proc. Natl Acad. Sci. USA* **90,** 7436–7440 (1993).

## METHODS

**Cell lines.** Human embryonic kidney cell line (HEK293) and neuroblastoma cells (SHSY-5Y) were cultured in DMEM containing 10% fetal bovine serum (FBS) in an atmosphere of 5% $CO_2$. Hippocampal neurons were prepared from 18-day-old rat embryos. Neurons were cultured at 37 °C in a humidified 5% $CO_2$ atmosphere with medium replenishment after 6 days, and used after 11 days of culture in all experiments.

**Animals.** Female Wistar rats (Charles River) were housed in diurnal lighting conditions (12 h darkness and 12 h light) and fasted overnight but allowed free access to water before the experiment. Experiments were carried out according to international guidelines for animal research and the experimental protocol was approved by the Animal Care Committee of the University of Naples.

**Plasmids and transfection** . Vectors encoding the Flag–praja2, GFP–praja2 and GST–praja2 were purchased from Genecopeia. Flag–praja2rm and Flag–praja2 mutants were generated by site-directed mutagenesis (GenScript), whereas praja2-deletion mutants and GST fusions were generated by PCR with specific oligonucleotide primers and subcloned into the same vector of wild-type praja2 cDNA. HA-tagged ubiquitin has been previously described[21,22]; epitope-tagged RIα and RIIα/β vectors have been previously described[21]. SMARTpool siRNAs targeting distinct segments of coding regions of praja2 and RIIα/β were purchased from Dharmacon and Sigma.

The following are the siRNA sequences (Thermo Scientific; LU-006916-00-10) targeting human praja2: sequence 1: 5′-GAAGCACCCUAAACCUUGA-3′; sequence 2: 5′-AGACUGCUCUGGCCCAUUU-3′; sequence 3: 5′-GCAGGAGGGUAUCAGACAA-3′; sequence 4: 5′-GUUAGAUUCUGUACCAUUA-3′.

The following are the siRNA sequences (Thermo Scientific; MQ-099442-00-0010) targeting rat neurodap1: sequence 1: 5′-GGCACUAGAAGAACGCUUA-3′; sequence 2: 5′-GUAGAGAGAUAUGCUGAUC-3′; sequence 3: 5′-GAAUGGAAUUGUGUUGGUU-3′; sequence 4: 5′-GCACGAGGCUAAGCAAAGA-3′.

For rescue experiments, we used siRNAs targeting the 3′-UTR (untranslated region) of human praja2 cDNA that do not alter the levels of Flag–praja2 (Sigma; SASI_Hs01_00214986: 5′-CACAAACCUUGUGUCUCAA-3′). Similarly, we used siRNAs targeting the 3′-UTR of human PRKAR2A (Thermo Scientific, A-007671-14: 5′-GCAGUUUGUAUGAAUGAAU-3′) and human PRKAR2B (Thermo Scientific, A-007673-14: 5′-UUAGAAUGUUAAUUGGAUA-3′). As a control, we used a non-targeting siRNA (Thermo Scientific, D-001810-02: 5′-UGGUUUACAUGUUGUGUGA-3′). siRNAs were transiently transfected using Lipofectamine 2000 (Invitrogen) at a final concentration of 100 pmol ml$^{-1}$ of culture medium.

**Antibodies and chemicals.** Rabbit polyclonal antibodies directed against RIIβ, RIIα, RIα and PKAc were purchased from SantaCruz and BD Transduction, and used at working dilutions of 1:300 (for immunostaining) and 1:1,000 (for immunoblot); extracellular signal-regulated kinase 2 (ERK2) (dilution 1:3,000), haemagglutinin epitope (HA.11, dilution 1:1,000), GST (dilution 1:5,000) and CaMKIIα (dilution 1:300) were purchased from SantaCruz; α-tubulin, Flag and Myc epitopes (dilutions 1:3,000 for immunoblot and 1:400 for immunostaining) were purchased from Sigma; phospho-Ser 133-CREB (dilution 1:1,000 for immunoblot and 1:200 for immunostaining) and CREB (dilution 1:1,000) were purchased from Millipore; two distinct polyclonal antibodies directed against human praja2 were generated in rabbit using the following epitopes: (1) residues 480–631; (2) residues 60–250. The two antibodies gave similar immunoblotting (dilution 1:500) and immunostaining (dilution 1:300) patterns. Forskolin, isoproterenol and cAMP were purchased from Sigma.

**Immunoprecipitation and pulldown assay.** Cells were homogenized and subjected to immunoprecipitation and immunoblot analyses as described previously[22]. GST fusions were expressed and purified from BL21 (DE3) pLysS cells. GST or GST–praja2 beads (20 µl) were incubated with 2 mg of cell lysate or with *in vitro* translated [$^{35}$S]-labelled R subunits in 200 µl lysis buffer (150 mM NaCl, 50 mM Tris-HCl at pH 7.5, 1 mM EDTA and 0.5% Triton X-100) in rotation at 4 °C overnight. Pellets were washed four times in lysis buffer supplemented with NaCl (0.4 M final concentration) and eluted in Laemmli buffer. Eluted samples were immunoblotted with the indicated antibody.

***In vitro* kinase assay and RII-overlay analysis.** Flag-tagged praja2 and Flag–praja2$^{S342A,T389A}$ mutant transiently expressed in HEK293 cells were immunoprecipitated with anti-Flag antibody. The precipitates were washed twice in kinase buffer (10 mM $MgCl_2$, 20 mM HEPES, at pH 7.4) and resuspended in the same buffer (50 µl) containing 10 µM ATP, 10 µCi of [$\gamma$-$^{32}$P ]ATP (Amersham), 100 µM cAMP and 10 units of purified PKAc (Sigma). Following incubation at 30 °C for 10 min, samples were washed three times in kinase buffer, resuspended in Laemmli buffer and loaded on an SDS–polyacrylamide electrophoresis gel. Phosphorylated proteins were visualized by autoradiography. RII-overlay assay was carried out as previously described[32], with the exception that RIIβ-binding proteins were visualized by immunoblotting the filter with anti-RIIβ antibody.

***In vitro* ubiquitylation assay.** [$^{35}$S]-labelled R subunits of praja2 were synthesized *in vitro* using a TnT Quick coupled transcription/translation system (Promega) in the presence of 45 µCi of [$^{35}$S]-labelled methionine. The ubiquitylation assay was carried out as described previously[22].

**siRNA administration into the rat brain.** All rats, anaesthetized with chloral hydrate (400 mg kg$^{-1}$, intraperitoneally), were put on a stereotaxic frame. A 23 g stainless-steel guide cannula (Small Parts) was implanted into the right lateral ventricle, the third ventricle, using the stereotaxic coordinates of 0.5 mm caudal to bregma, 2 mm lateral and 2.5 mm below the dura. The cannula was fixed to the cranium using dental acrylic and small screws. siRNAs targeting rat praja2 (10 µl from 250 µM stock) and control siRNAs (10 µl from 250 µM stock) were administered three times, 24 h, 12 h and 1 hour before isoproterenol stimulation. Rats were killed 30 min or 60 min later. Distinct brain regions (cortex, hippocampus and striatum) from the left and right hemispheres were isolated. Brain tissues were used for immunoblot analysis and RNA extraction.

**RNA purification and quantitative PCR analysis.** Total RNA was extracted with TRIzol reagent according to the manufacturer's protocol (Sigma). Two micrograms of the isolated RNA were reverse-transcribed with the Omniscript RT kit (Qiagen). Real-time PCR was carried out in triplicate in 20 µl reaction volumes using the Power SYBER Green PCR Master Mix (Applied Biosystems). PCR primers for human c-*fos* mRNA are the following: forward 5′-CGGGCTTCAACGCAGACTA-3′; reverse 5′-GGTCCGTGCAGAAGTCCTG-3′. For rat c-*fos* mRNA, we used the following primers: forward 5′-AGCATGGGCTCCCCTGTCA-3′; reverse 5′-GAGACCAGAGTGGGCTGCA-3′. 18S RNA was used as reference. Real-time PCR reactions were carried out in a MJ Mini Personal Thermal Cycler apparatus (Bio-Rad Laboratories). Melting curves were obtained by increasing the temperature from 60 to 95 °C with a temperature transition rate of 0.5 °C s$^{-1}$. Melting curves of final PCR products were analysed (OpticonMonitor 3 Bio-Rad).

**Confocal microscopy and image analysis.** Forebrain coronal vibratome sections were subjected to immunostaining after incubation with anti-RIIβ, anti-praja2 and anti-CaMKIIα antibodies. Immunofluorescence was visualized using a Zeiss LSM 510 Meta argon/krypton laser scanning confocal microscope. Four images from each optical section were averaged to improve the signal-to-noise ratio. A minimum of four sections per brain and four different samples per region were analysed. Cultured cells transiently transfected with expression vectors were fixed and immunostained with anti-RIIα/β, anti-PKAc, anti-Flag or anti-praja2 antibodies. Confocal analysis was carried out as above. Quantification of the immunofluorescent images and correlation (Pearson's) coefficient were calculated by Image-J software.

**cAMP precipitation.** β2AR-HEK293 cells transiently overexpressing praja2 fusions were treated with indicated stimuli, lysed and subjected to precipitations with Rp-8-AHA-cAMP agarose resin (Biolog) for 2 h. In this assay, binding of R subunits to the resin-coupled cAMP analogue results in re-association of PKAc:R subunits. We elevated endogenous cAMP levels with Fsk or through activation of the stably expressed beta2-adrenergic receptor (β2AR) by isoproterenol before cell lysis. As a control, we added an excess of cAMP (5 mM) to mask the cAMP-binding sites in the R subunits for precipitation. Resin-associated complexes were washed with the lysis buffer and subjected to immunoblot analysis.

**Bioluminescence assays.** β2AR-HEK293 cells transiently overexpressing praja2 fusion proteins and the Rluc-PCA-tagged R and PKAc subunits in a ratio of 4:1:1 were treated with Fsk (50 or 100 µM) for 15 min. After treatment (in 24-well plates), cells were resuspended in 350 µl of phosphate buffered saline (PBS). Cell suspension (100 µl) was transferred to 96-well plates and subjected to bioluminescence analysis using the LMax II$^{384}$ luminometer as described previously[36] (Molecular Devices). For the re-association (Fig. 5m), we used osteosarcoma cell line U2OS. Cells grown in 12-well plates transiently overexpressing different praja2 fusions and the Rluc-PCA-tagged RII and PKAc subunits in a ratio of 4:1:1 were treated with Fsk (50 µM, 30 min). Following treatment, cells were washed twice with PBS and incubated for a further 60 min at 37 °C in DMEM with 10% FBS. After two further wash steps with PBS, cells were scraped and 200 µl cell suspensions were transferred to 96-well plates for bioluminescence analysis.

**Electrophysiology.** All animal procedures were in compliance with the European Council Directive (86/609/EEC). Parasagittal hippocampal slices (400 µm) from rats treated with siRNAs targeting praja2 and control siRNA were kept submerged at 30 °C and superfused (2–3 ml min$^{-1}$) with oxygenated (95% $O_2$, 5% $CO_2$) artificial cerebrospinal fluid (ACSF) containing (mM): 124 NaCl, 2.5 KCl, 1.25 $NaH_2PO_4$,

DOI: 10.1038/ncb2209

1.3 $MgSO_4$, 2.4 $CaCl_2$, 26 $NaHCO_3$ and 10 glucose. Presynaptic stimulation was applied to the medial perforant pathway of the dentate gyrus using a bipolar insulated tungsten wire electrode, and field excitatory postsynaptic potentials were recorded at a control test frequency of 0.033 Hz from the middle one-third of the molecular layer of the dentate gyrus with a glass microelectrode. The transient E-LTP was induced by one train of HFS (1 s train at 100 Hz) in the perforant pathway of the dentate gyrus, whereas long-lasting L-LTP was induced with TBS consisting of nine bursts of four pulses at 100 Hz, 200 ms interburst interval, 5 min intertrain interval[40]. All solutions contained 100 μM picrotoxin (Sigma) to block $GABA_A$ (γ-aminobutyric acid A)-mediated activity.

**Statistics.** Electrophysiological data are presented as mean ± s.e.m. and are normalized with respect to a 20 min baseline. *n* indicates the number of hippocampal slices. Statistical significance for all of the experiments presented was evaluated by an unpaired Student *t*-test. Values are expressed as means ± s.e.m. Statistical significance was accepted at the 95% confidence level ($P < 0.05$).

nature cell biology



DOI: 10.1038/ncb2209

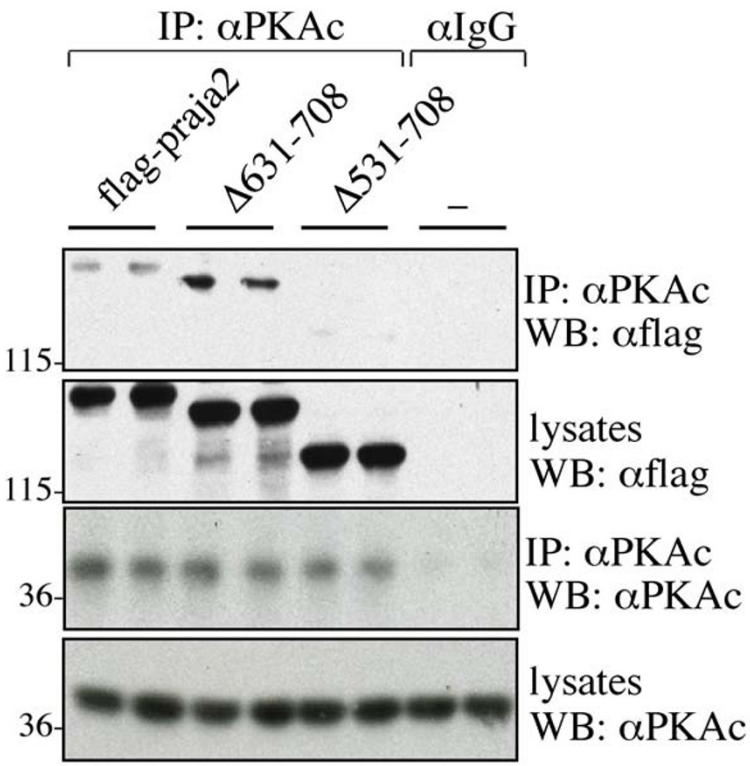


**Figure S1** Lysates from cells transfected with flag-praja2 (either wild type or deletion mutants) were immunoprecipitated with anti-PKAc antibody. The precipitates and an aliquot of lysates were immunoblotted with anti-PKAc and anti-flag antibodies.

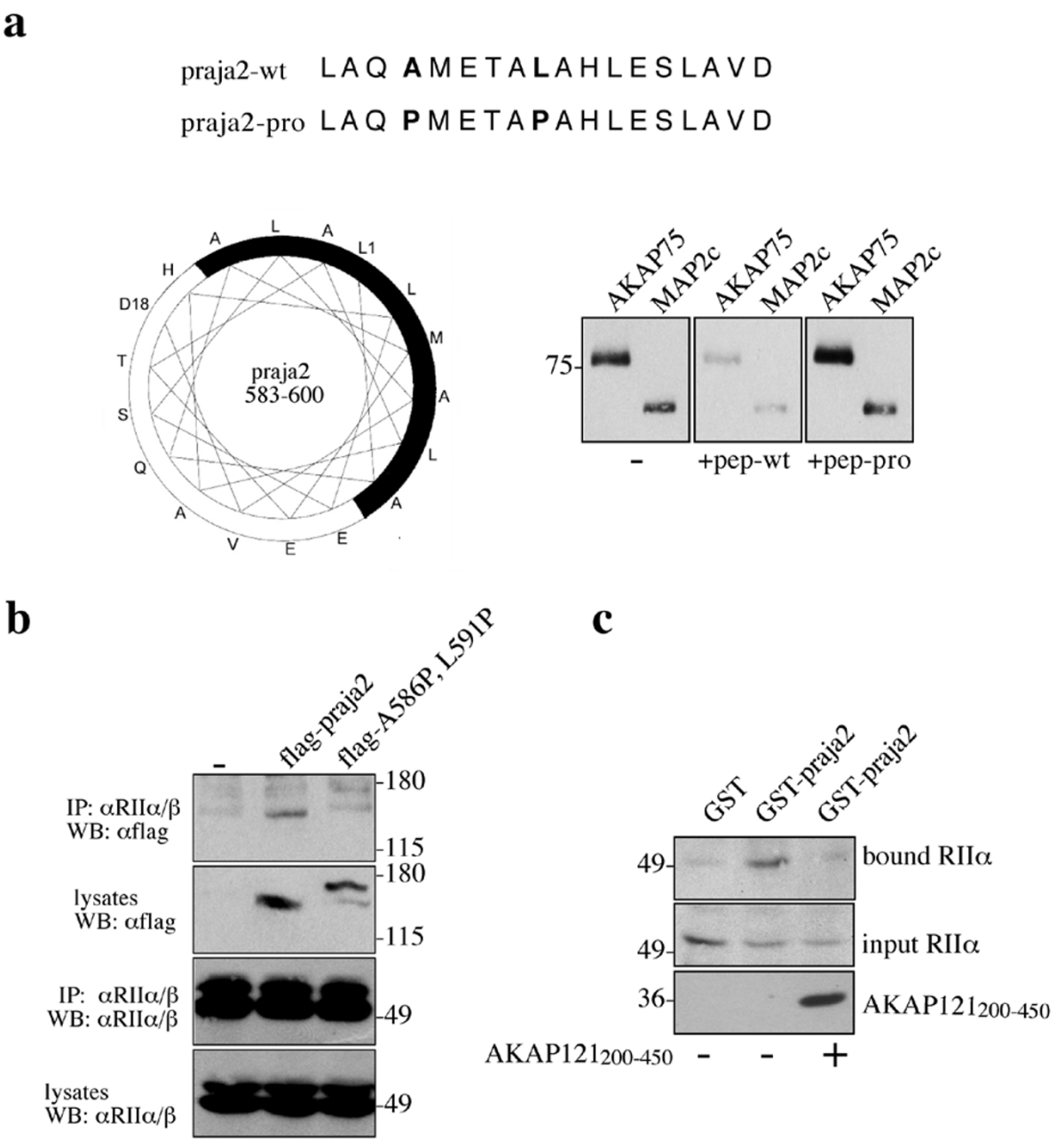


**Figure S2** (**a**) Primary sequence of residues 583-600 of human praja2 along with helical wheel representation. Hydrophobic face is in bold. 1 mg of recombinant MAP2c and AKAP75 were loaded on SDS-PAGE, transfered to nylon membrane and overlayed with purified RIIb (200ng/ml), in presence or absence of praja2 peptide(1mM), either wt (pep-wt) or proline mutant (pep-pro). After extensive washes in binding buffer, bound-RIIb was revealed by immunoblot analysis with anti-RIIb antibody. (**b**) flag-praja2 and mutant flag-A586P,L591P were transiently transfected in HEK293 cells. Lysates were immunoprecipitated with anti-RIIa/b antibody. The precipitates and an aliquot (100mg) of lysate were immunoblotted with the indicated antibodies. (**c**) HEK293 lysates were subjected to pull down assay using GST-praja2. Where indicated, molar excess (20mg) of recombinant AKAP121 polipeptide ($AKAP121_{200-450}$) was added to the lysate. Bound and input fractions were immunoblotted with anti-RII and anti-AKAP121 antibodies.

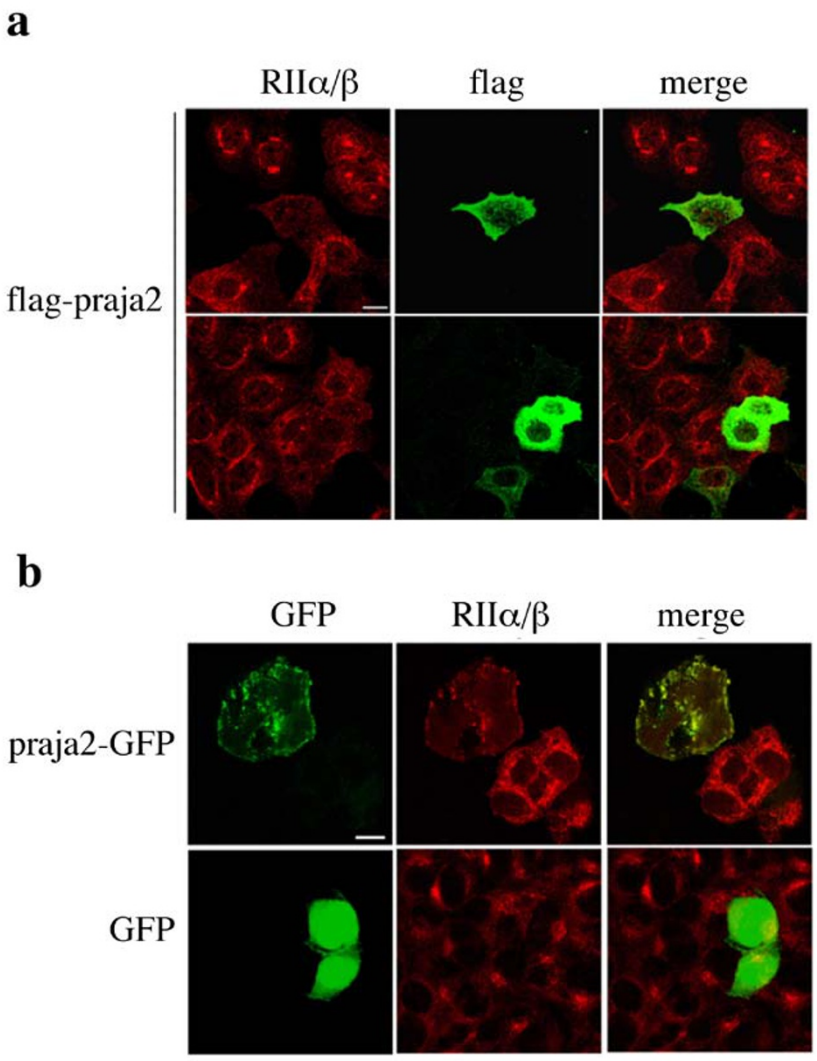


**Figure S3** (**a**) Human neuroblastoma cells (SHSY) were transiently transfected with flag-praja2. 24 hours from transfection, cells were fixed and doubly immunostained with anti-RIIa/b and anti-flag antibodies. Fluorescent images were collected and analyzed by confocal microscopy. A merged composite is shown. Scale bar: 20mm. (**b**) cells were transiently transfected with praja2-GFP (upper panels) or GFP (lower panels). Immunostaining was performed with anti-RIIa/b. Scale bar: 20mm.

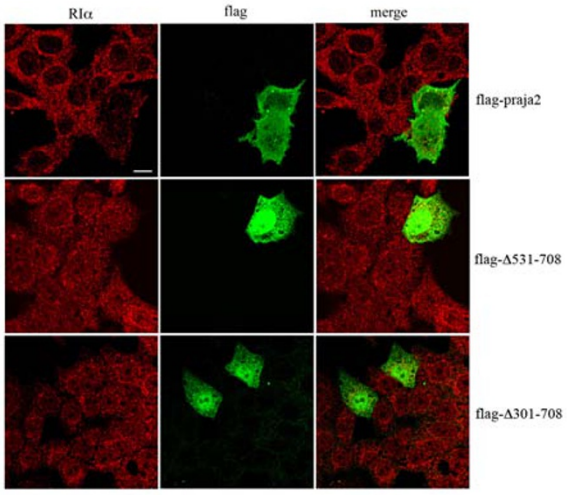


**Figure S4** Human neuroblastoma cells (SHSY) were transiently transfected with flag-praja2 or its deletion mutants (Δ531-708 and Δ301-708). 24 hours from transfection, cells were fixed and immunostained with anti-RIa and anti-flag. Fluorescent images were collected and analyzed by confocal microscopy. A merged composite is shown. Scale bar: 20 μm.

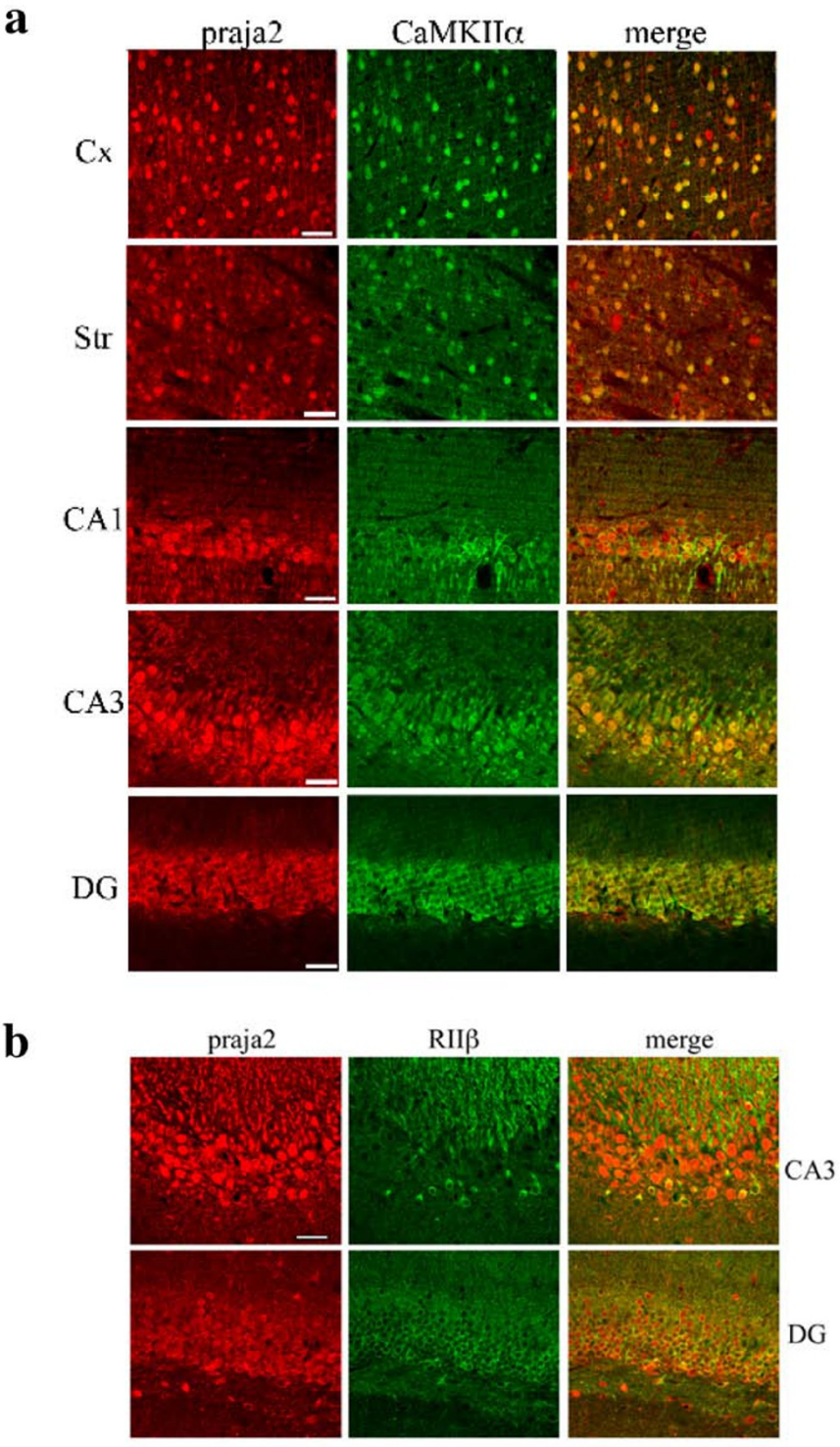


**Figure S5** Distribution of praja2, CaMKIIa and RIIb in the rat brain. Sections from cerebral cortex (Cx), striatum (Str), hippocampus (CA1, CA3) and dentate gyrus (DG) were doubly immunostained with anti-praja2 and anti-CaMKIIa (**a**) or anti-RIIb (**b**) antibodies. Images were collected by confocal microscopy. Bar= 50 mm.

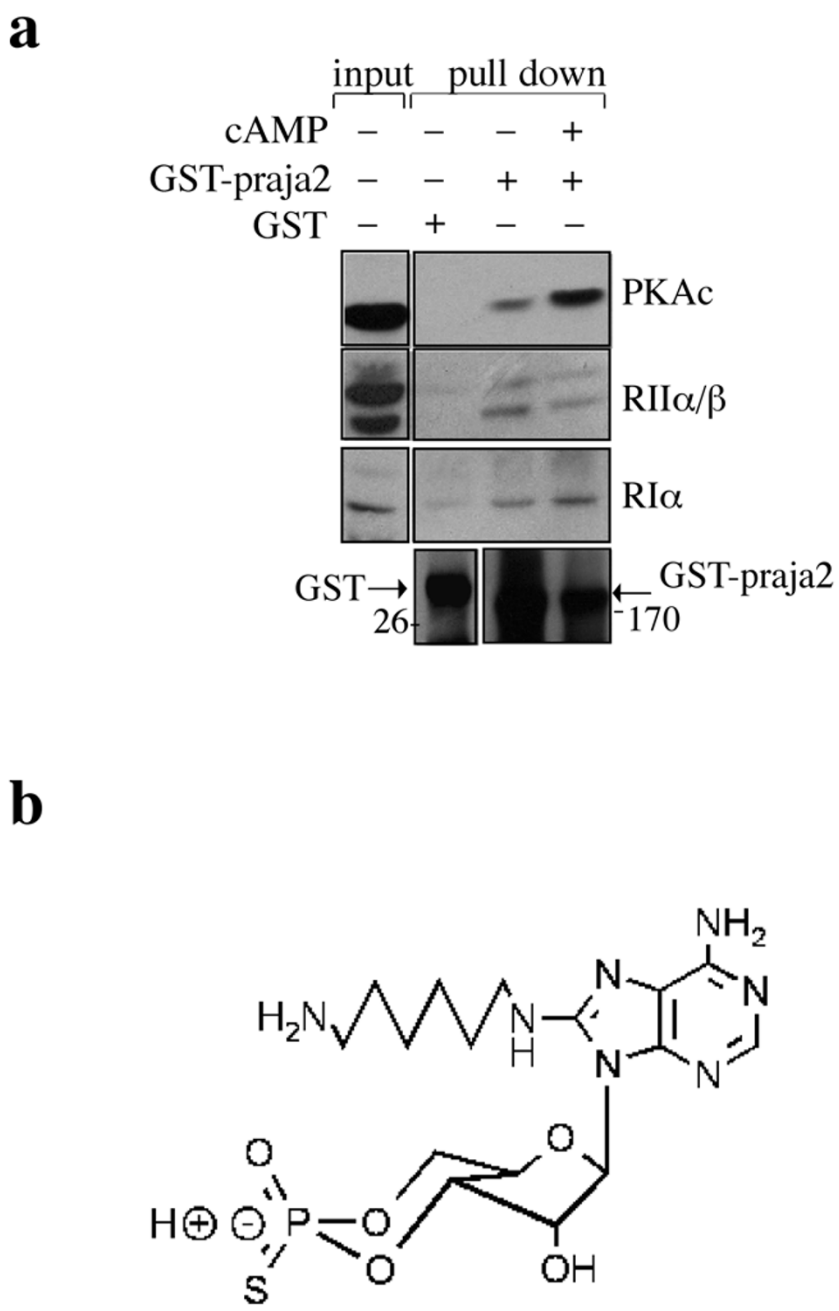


**Figure S6** (**a**) Cell lysates (1 mg) were incubated with purified GST-praja2 or GST polypeptide. Where indicated, the lysate was pretreated with cAMP (250 mM). GST beads-bound and input (10%) fractions were immunoblotted with the indicated antibodies. (**b**) Schematic structure of the cAMP analog, Rp-8-AHA-cAMP.

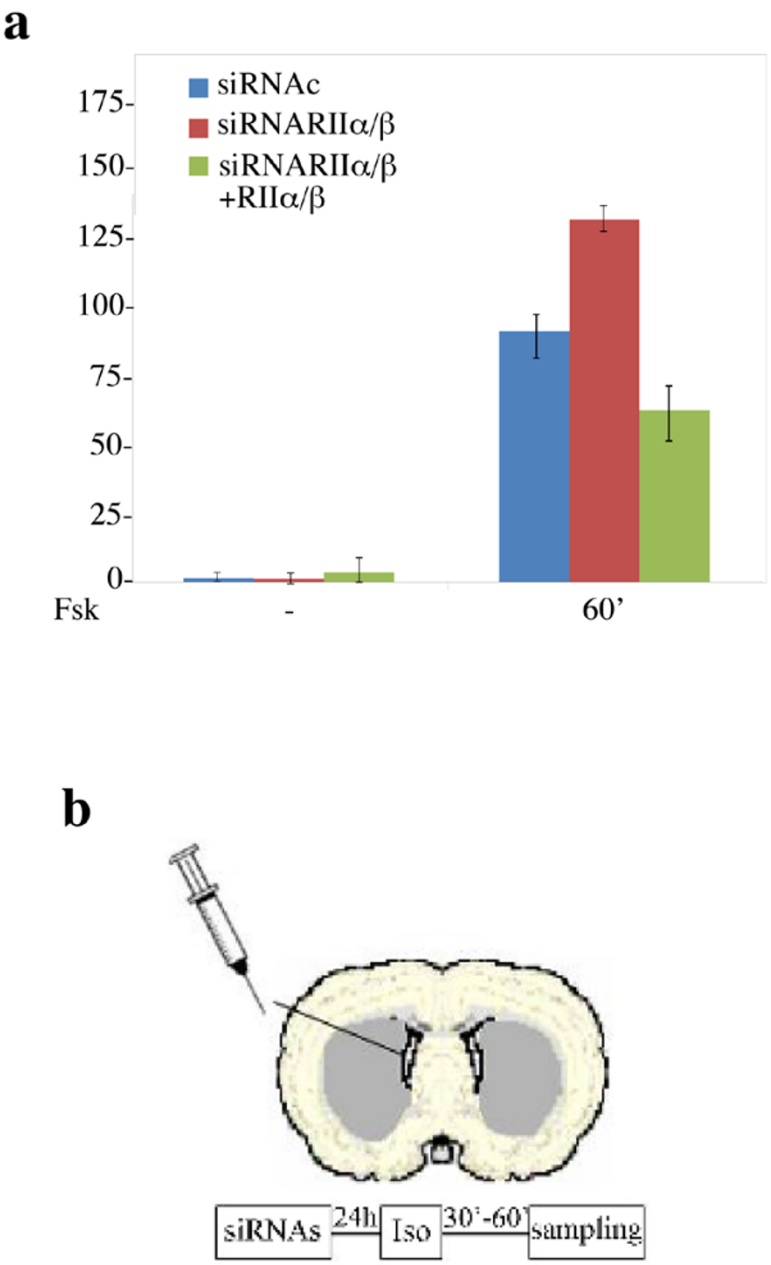


**Figure S7** (**a**) Quantitative RT-PCR analysis of c-fos mRNA accumulationin cells transiently transfected with siRNAc or a mixture of 3'UTR-siRNARIIa and 3'UTR-siRNARIIb and stimulated with forskolin for 60 min. Data represent a mean value from two independent experiments made in duplicate. Where indicated, vectors encoding for RIIa-HA and RIIb-myc where included in the transfection mixture. (**b**) Schematic diagram showing intraventricular siRNA administration in rat brain. Three sequential siRNAs infusions were employed (time points: 0 h, 10 h, 22 h).

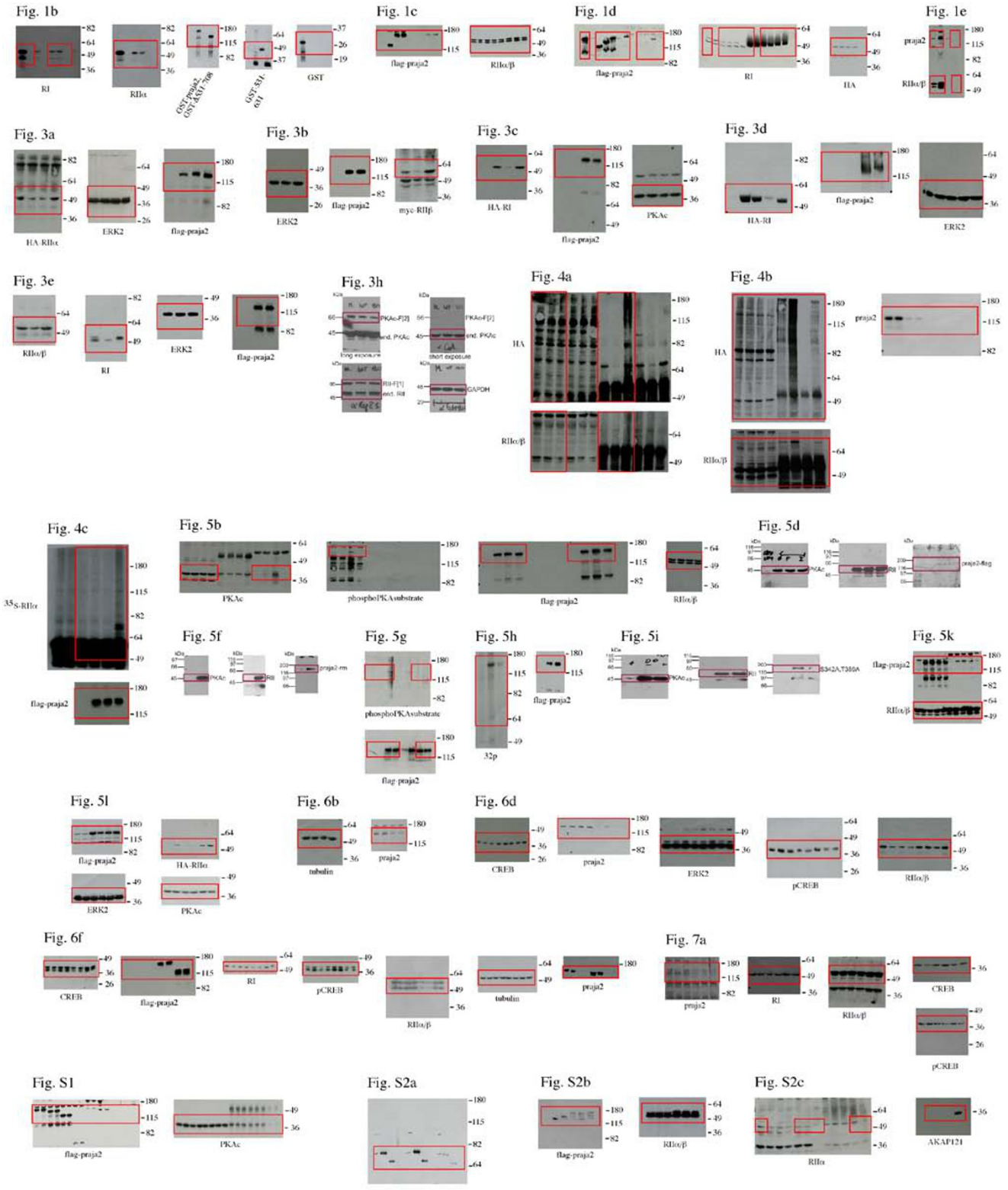


**Figure S8** Full scans of western blots presented. Blots not shown were cut into strips and subsequentely probed with specific antibodies. The area used as data in the figures are indicated by the red boxes. Molecular weight markers are included.